Computational Approaches to Protein Structure Prediction

by

Zerrin Işık

Submitted to the Graduate School of Engineering and Natural Sciences
in partial fulfillment of
the requirements for the degree of
Master of Science

Sabancı University
Spring 2003

Computational Approaches to Protein Structure Prediction

APPROVED BY

Assist. Prof. A. Berrin Yanıkoğlu   ....
(Thesis Supervisor)

Assist. Prof. O. Uğur Sezerman   ....
(Thesis Co-Supervisor)

Assist. Prof. Hakan Erdoğan   ....

Assoc. Prof. Canan Baysal   ....

Assist. Prof. Hüsnü Yenigün   ....

DATE OF APPROVAL: ....

to Bioinformatics volunteers

Acknowledgments

During my graduate education at Sabancı University, many people helped me to complete my graduate program. First of all, I would like to thank my advisor Berrin Yanıkoğlu who encouraged me to work on projects in which I have had most interest. I am thankful to her for giving useful advice, for sharing experiences, and most importantly for teaching me how think analytically. I would also like to thank my co-adviser, Uğur Sezerman. He first introduced me to Bioinformatics and its fundamental topics. I would like to thank Hakan Erdoğan for his help on the HMM tool and providing me with a new point of view about the project.

I want to thank my officemates, İlknur Durgar and Alisher Kholmatov. Although we were working on different projects, we always supported each other. I want to thank to Thomas Bechteler for his quick and very useful assistance on LaTeX and, of course, for his friendship. Lastly, I should not forget to thank my friend Ömür Kayıkçı since she encouraged and offered her hand to save the world together.

Lastly, a special thank you goes to my family. They have always given me their unconditional love and supported me in my life and education. My heartfelt thanks for *my beloved partner Buğra Sökmen.* Even though I could not express his love and support with a couple of words, he has tried to make the life easier for me during the thesis work and the writing of my thesis. He has always been om my side since the beginning of the our friendship. This thesis is dedicated to my family.

Abstract

One of the most promising problems in bioinformatics is still the protein folding problem which tries to predict the native 3D fold (shape) of a protein from its amino acid sequence. The native fold information of proteins provide to understand their functions in the cell. In order to determine the 3D structure of the huge amount of protein sequence, the development of efficient computational techniques is needed.

The thesis studies the computational approaches to provide new solutions for the secondary structure prediction of proteins. The 3D structure of a protein is composed of the secondary structure elements: α-helices, β-sheets, β-turns, and loops. The secondary structures of proteins have a high impact on the formation of their 3D structures. Two subproblems within secondary structure prediction have been studied in this thesis.

The first study is for identifying the structural classes (all-α, all-β, α/β, $\alpha+\beta$) of proteins from their primary sequences. The structural class information could provide a rough description of a protein's 3D structure due to the high effects of the secondary structures on the formation of 3D structure. This approach assembles the statistical classification technique, Support Vector Machines (SVM), and the variations of amino acid composition information. The performance results demonstrate that the utilization of neighborhood information between amino acids and the high classification ability of the SVM provides a significant improvement for the structural classification of proteins.

The second study in thesis is for predicting one of the secondary structure element, β-turns, through primary sequence. The formation of β-turns has been thought to have critical roles as much as other secondary structures in the protein folding pathway. Hence, Hidden Markov Models (HMM) and Artificial Neural Networks (ANN) have been developed to predict the location and type of β-turns from its amino acid sequence. The neighborhood information between β-turns and other secondary structures has been introduced by designing the suitable HMM topolo-

gies. One of the amino acid similarity matrices is used to give the evolutionary information between proteins. Although applying HMMs and usage of amino acid similarity matrix is a new approach to predict β-turns through its protein sequence, the initial results for the prediction of β-turns and type classification are promising.

Özet

Bioinformatik alanında, protein katlanma problemi çözüm bekleyen problemlerden birisidir. Burada amaç proteinin üç boyutlu yapısını proteinin amino asit bilgisini kullanarak belirleyebilmektir. Bir proteinin üç boyuttaki yapısını bildiğimiz zaman, onun hücre içindeki fonksiyonu hakkında da bilgi sahibi oluruz. Bir proteinin yapısının deneysel yollarla bulunması çok uzun zaman alabilmektedir. Bu nedenle yapısı bilinmeyen binlerce protein dizisinin yapısını belirleyebilmek için daha etkili hesaba dayalı teknikler geliştirilmelidir.

Bu tez çalışmasında proteinin ikincil yapısını tahminlemek amacıyla hesaba dayalı yaklaşımlar geliştirilmiştir. Proteinlerin üç boyutlu yapısı, ikincil yapı öğelerinden (α-helezonları, β-tabakaları, β-dönüşleri, ve döngüler) oluşmaktadır. Proteinin ikincil yapısının üç boyutlu yapısının oluşmasında büyük etkileri bulunmaktadır. Bu nedenle bu tez çalışması kapsamında proteinin ikincil yapısının tahminlenmesi amacıyla iki farklı yaklaşım çalışılmıştır.

İlk yaklaşım, proteinlerin yapısal sınıflarını amino asit dizisi yardımıyla belirlemek için geliştirilmiştir. Proteinin yapısal sınıf bilgisi onun üç boyutlu katlanmış şekli hakkında fikir verebilmektedir, çünkü proteinlerin ikincil yapısının onların alacağı katlanma şekli üzerinde büyük etkisi bulunmaktır. Bu yaklaşım içersinde, istatiksel sınıflandırma tekniklerinden birisi olan Destekçi Vectör Makinası ve çeşitli amino asit nitelik bilgileri birleştirilmiştir. Destekçi vectör makinasının yüksek sınıflandırma yeteğine sahip olması ve amino asitler arasındaki komşuluk bilgisinin kullanılması performans sonuçlarında iyileşmeye sebep olmuştur.

Tez projesi içersinde yer alan ikinci çalışma, proteinlerin ikincil yapı öğelerinden olan β-dönüşlerinin yine amino asit bilgisinden yararlanılarak tahminlenmesidir. Diğer ikincil yapı öğeleri kadar β-dönüşlerinin oluşmasının da proteinin katlama aşamalarında önemi olduğu düşünülmektedir. Bu sebeple β-dönüşlerinin protein içersindeki yerini belirleyebilmek ve tiplerini tespit edebilmek amacıyla saklı Markov modeline ve yapay sinir ağına dayanan yaklaşımlar geliştirilmiştir. β-dönüşleri ve

diğer ikincil yapı öğeleri arasındaki komşuluk bilgisinin verilebilmesi uygun saklı Markov model topolojilerinin oluşturulmasıyla sağ- lanmıştır. Proteinler arasındaki evrimden kaynaklan ortak bilgiler de bir çeşit amino asit benzerlik matrisi ile sisteme verilmektedir. β-dönüşlerinin yerlerini tahminleme probleminde saklı Markov modellerinin ve amino asit benzerlik matrisinin kullanılması yeni bir yaklaşımdır. Bu çalışmada β-dönüşlerinin yerinin ve tiplerinin belirlenmesinde elde edilen ilk sonuçlar oldukça ümit verici olmuştur.

Table of Contents

List of Figures

List of Tables

Chapter 1

Introduction

The past decade has produced many discoveries in the field of biology; particularly, the completion of the sequencing of the human genome, was a major breakthrough, which offers a huge sequence of data waiting for processing. There are many applications for sequence analysis, i.e., gene finding, protein secondary structure prediction, protein fold prediction, protein function prediction, and interactions of different type of proteins. Although scientists are trying to find solutions using both experimental and computational methods, the cost and time limitations inherent in experimental methods have increased the importance of the development of computational solutions. Hence, computational biology has a key role to explore in the working mechanism of the cell machine.

Figure 1.1: The illustration of the protein folding mechanism.

This thesis project focuses on the **protein folding problem** which attempts to predict the 3D structure (native state) of a protein given its composition (amino acid content). Proteins, built from the same amino acid content, always fold to the

same native state (Figure 1.1). Thus, two crucial questions of the protein folding problem should be examined: how a protein folds its native state and how we can predict that native state from the amino acid sequence.

Research concerning the native folded state of a protein has great potential to provide many biological events; since, the 3D structure of a protein gives functional information about that protein and one of the fundamental aims of biology is to understand the function of proteins. Knowledge about the function of proteins provides an understanding of biochemical processes in living beings, the characterization of genetic diseases, the implementation of designer drugs, and so on. Despite the years of research, the wide variety of approaches that have been utilized in an attempt to solve the protein folding problem, it remains an open problem for computational biology. In this thesis project, several different computational techniques are applied to extend the solutions for the protein folding problem.

1.1 Overview of Protein Structures

Proteins are complex molecules which perform critical tasks in the cell. Each type of cell has different kinds of proteins which determine the cell's function. They are composed of amino acids chains whose length ranges between fifty and five thousand. There are twenty different types of amino acids which share the same **core region**. The carbon, hydrogen, nitrogen, oxygen atoms constitute the core region of an amino acid (see Figure 1.2).

Several different protein conformations are possible due to the rotation of the protein chain (marked with ψ, ϕ angles in Figure 1.2) about the main carbon (C_α) atom. When all amino acids make bonds in protein chain, the connected region of the C_α atoms is called the **protein backbone**.

The main criteria to distinguish two amino acids is the **R side chain** of each one. The protein's properties are determined by the nature of the side chains. In particular, amino acid side chains can be polar, hydrophobic, or charged. The side chain difference between amino acids arises from the chemical properties. Polar amino acids tend to be present on the surface of a protein where they can interact

Figure 1.2: The structure of two amino acids in a polypeptide chain. Each amino acid is encircled by a hexagon. The backbone of the protein chain is shown by a rectangle.

Amino Acid Code	Name	Chemical Group
A	Alanine	Hydrophobic
V	Valine	
F	Phenylalanine	
P	Proline	
M	Methionine	
I	Isoleucine	
L	Leucine	
D	Aspartic Acid	Charged
E	Glutamic Acid	
K	Lysine	
R	Arginine	
S	Serine	Polar
T	Threonine	
Y	Tyrosine	
H	Histidine	
C	Cysteine	
N	Asparagine	
Q	Glutamine	
W	Tryptophan	
G	Glycine	-

Table 1.1: Types of amino acids according to their chemical properties.

with aqueous environments. On the other hand, hydrophobic amino acids tend to reside within the center of the protein where they can interact with similar hydrophobic neighbours. The charged amino acids have unbalanced side chains; hence, they contain an overall positive or negative charge. The polar, charged, and hydrophobic amino acid names are listed in Table 1.1.

The amino acid sequence of a protein is called the **primary structure** of the protein. The common idea is that the amino acid sequence of a protein has a significant effect on the fold of a protein. The fold of a protein states the 3D structure of the protein. Each protein has a unique 3D structure; however, different proteins can have the same fold. Although the number of different sequences is growing with the size of the protein (20^N), there are roughly 700 unique folds found so far [65]. So, the folding process should have some principles to get the similar folds in spite of having different amino acid sequences. One way to understand the fundamentals of protein folding is identifying the short regions, called **secondary structures**, in proteins. The secondary structure prediction can be an intermediate step in predicting the 3D structure.

The secondary structures consist of four different elements, α-helix, β-sheet, turn, and loop (see Figure 1.3). The α-helices and β-sheets compose the core region of proteins. The amino acids, whose space to move is limited, have a compact structure in the core region. The turns and loops are outside of the core region and contact with water, other proteins, and other structures. The amino acid substitutions in these regions are not as restricted as in the core region.

The α-**helix** is the most abundant type of secondary structure in proteins (see Figure 1.4). It is a helical structure formed by the bonding of backbone NH and CO atoms from residues (amino acids) at position **i** and **i+4**. These bondings, along the α-helix, lead to approximately 3.6 residues per turn of the helix. The R side chains of the amino acids are on the outside of the helix. The number of residues in an α-helix can vary from 4 to over 40. α-helices appear mostly on the surface of the protein core, with the hydrophobic amino acids being inside of the α-helix and the polar and charged ones being outside.
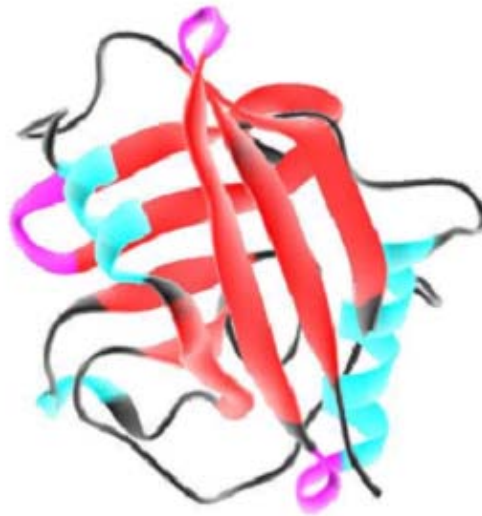
Figure 1.3: The 3D structure of a protein. The secondary structure elements have different colors. The α-helix, β-sheet, turn, loop structures are shown in light blue, red, pink, and grey, respectively.
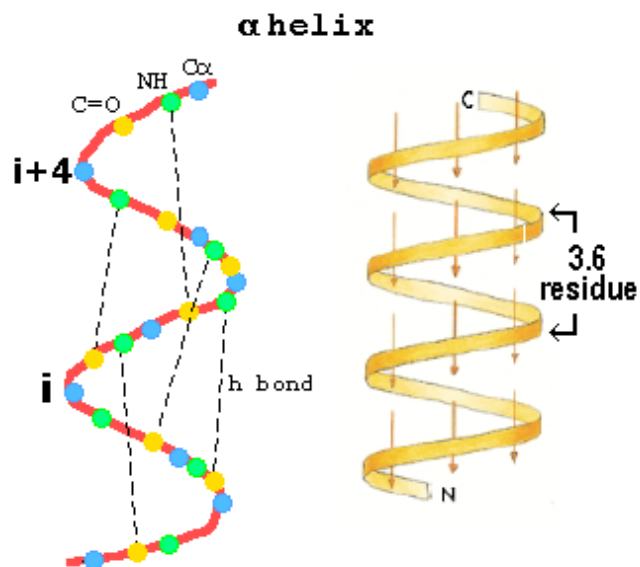
Figure 1.4: The α-helix secondary structure. The backbone of the chain is shown in red. The Cα atoms and the C=O and NH groups are shown in blue, yellow, and green, respectively. In the α-helix, each C=O group at position i in the sequence is hydrogen-bonded with the NH group at position i+4. (This figure is taken from Mount [61]).

The amino acid contents can help predict a α-helix region. Alanine, leucine, methionine, and glutamic acid are frequently seen in the α-helix formation. However, proline, glycine, serine, and tyrosine are hardly found in the α-helix. Proline is known especially as α-helix breaker, due to its destabilizing effect on the bonds.

The β-**sheets** are another secondary structure found in proteins (see Figure 1.5). They are built up from several interacting regions of the main chain which is called **strands**. The strands align so that the NH group on one strand can bond to the CO group on the adjacent strand. The β-sheet consists of parallel or antiparallel alignments of strands. In antiparallel β-sheets; the strands that are involved in hydrogen bonds run in opposite directions, one runs in the C to N direction, while the other runs in the N to C direction. In parallel β-sheets, both strands that are involved in hydrogen bonding run in the same direction. Each amino acid in the interior strands of the sheet forms two H bonds with neighboring amino acids, whereas each amino acid on the outside strands forms only one bond with an interior strand. The prediction of β-sheets is more difficult than α-helix due to the long range interactions between strands.
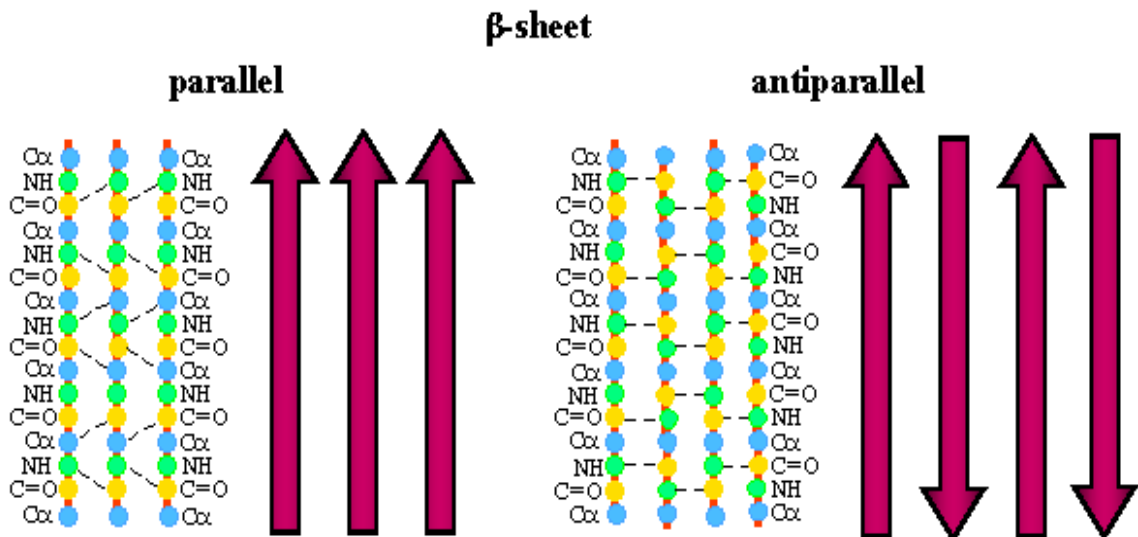
Figure 1.5: The β-sheet structure. The backbone of the chain is shown in red. The Cα atoms and the C=O and NH groups are shown in blue, yellow, and green, respectively. The β-sheet is made up of strands that are portions of the protein chain. The strands may run in the same (parallel) or opposite (antiparallel) directions. (This figure is taken from Mount [61]).
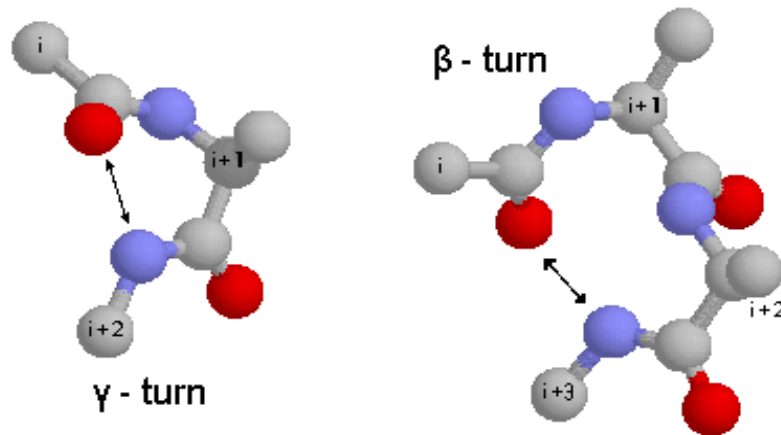
Figure 1.6: The γ-turn and β-turn secondary structures. In a γ-turn, a hydrogen bond exists between residue i (CO) and residue i+2 (NH). In β-turn, a hydrogen bond exists between residue i (CO) and residue i+3 (NH).

Turns are small secondary structures according to α-helices and β-sheets (see Figure 1.6). Turns are located primarily on the protein surface and accordingly contain polar and charged residues. One-third of all residues in proteins are contained in turns that serve to reverse the direction of the chain. They are classified according to their length, varying from two to six amino acids.

The regions rather than β-sheets, α-helices, and turns are called **loops**. These loop structures contain between 6 and 16 residues and are compact and globular in structure. They reside on the surface of the structure and interact with the surrounding environment and other proteins. The amino acids in the loops are frequently polar and charged.

The 3D structure of a protein is composed of secondary structure elements. The determination of the protein 3D structure is troublesome and not always a feasible process using experimental methods, such as x-ray crystallography or nuclear magnetic resonance spectroscopy; since, these methods are expensive, time consuming, labor-intensive, and not applicable to all types of proteins due to physical constraints. The gap between the sequences with known and unknown structures has increased after the completion of the sequencing of human genome. Hence, the necessity to explore the new fast, easy, and effective computational methods for determining 3D structures is obvious.

1.2   History of Computational Methods

Much work has been done in predicting the structure of a protein from its amino acid sequence. The well-known research topic is the protein folding problem that is a difficult problem due to the vast number of possible conformations that could be adopted. Therefore, several different approaches to protein structure prediction have been designed.

Each protein has a unique fold and gets the same fold from the same sequence every time because its stable conformation minimizes energy of the protein. The physical approach of modelling all the forces and energy involved in protein folding is the most straight forward and successful method on predicting the 3D native structure. However, this solution is very time consuming due to searching the vast conformational space for a global energy minimum; the calculations take more than a year on a supercomputer to find a known minimum energy configuration of a small protein.

As the physical approach takes inhibitively long, computational approaches have been studied massively and still much more work needs to be done to find more efficient and reliable computational methods. We will give the most important computational approaches for the protein folding problem in the next sections.

1.2.1   Homology Modelling

Homology modelling is one of the comparative techniques. The protein sequence of an unknown structure is compared to sequences of known structures in the comparative approaches. Therefore, the comparative approaches are constrained by the number of known structures.

The homology modelling is based on the structure which conserved in evolution. The sequence may change during the evolution (mutations, deletions, insertions); however, the structures of homologous proteins are conserved. When protein sequences share a significant sequence similarity, they are called **homologous** proteins which are assumed to have close evolutionary ancestry.

The databases of sequences of known structure are searched to find similar

(homologous) sequences. The alignment of the homologous sequences is used as input for the homology modelling program. It uses the alignment of proteins to generate spatial constraints (distance between non-adjacent residues, the dihedral angles between adjacent residues, and so on) on the target sequence. Finally, the homology modeler generates a possible conformation of the protein and optimises it with respect to the spatial constraints.

The most commonly used homology modelling programs are the Modeler and WHAT IF [56, 91].

1.2.2 Threading

Threading attempts to find a known fold that the given sequence with unknown structure could construct. Sometimes threading is called **fold recognition**.

The steps of measuring the best fitted fold in the whole fold space can be summarized in the following: Firstly, the target sequence (with an unknown fold) is threaded through all the existing folds. Then, a score function should be assigned to make a comparison between all threaded folds. The contact potential and sequence profile method are the most common techniques to compute the score function. After that, a search strategy for the threading should be determined. There exist many local minimas in the search space; hence, the search algorithm is a crucial part of the threading. There are several different heuristics to search the whole fold space, i.e., double dynamic programming [37], Gibbs sampling algorithm [7], branch and bound algorithm [48], recursive dynamic programming [86], and neural network [38].

The most successful threading servers are GenThreader and Fugue [38, 83].

1.2.3 Secondary Structure Prediction

The detection of the secondary structures of a protein would give useful information to determine the 3D structure of that protein. Therefore, the prediction of the secondary structures of proteins can be one subgoal within the protein folding problem. There exist multiple generations of approaches to predict the secondary structures

of proteins. These approaches are explained below in detail; since the secondary structure prediction closely relates to the subtopics of this thesis.

The first generation of the secondary structure prediction approaches used the single amino acid compositions [6, 66, 84]. In other words, these approaches used the percentage of each amino acid in a given protein (e.g. %7 alanine, %3 proline, %6 cystine). Due to the small size of the known structure databases, the statistical results of these approaches were not realistic.

Along with increasing the size of the known structure databases, a second generation of prediction methods were developed. They computed the amino acid compositions for the longer segments to incorporate the neighboring information of amino acids. The scientists applied several different machine learning techniques to analyse the segments with long length. The multi layer neural networks were the most popular machine learning technique [31, 46, 54, 68]. The prediction performance of these methods was lower than 70% ; furthermore, they could not predict β-strands better than could random prediction. The reason for the limited prediction performance was that the training systems by using merely the local information; however, long range amino acid interactions have effects on the formation of the secondary structures like β-strands. If the long range effects had been included to the next generation of secondary structure prediction methods, would have played more important role in determining the 3D structure of proteins.

The third generation secondary structure prediction approaches have tried to combine machine learning techniques and evolutionary information. The sequence of a protein may change while the evolution but its structure is preserved. The different alignment techniques have been applied to consider the evolutionary information between proteins. The first usage of alignment information has been proposed first by Maxfield and Scheraga and by Zvelebil et al. [57, 96]. In the sequence alignment, two or more strings (amino acid segments) are aligned together in order to get the highest number of matching characters. Gaps may be inserted into a string in order to shift the remaining characters into better matches. The above research compiled predictions for each protein in an alignment, then averaged over all proteins. **Profiles** which are compiled from the multiple sequence alignments

are the better way of considering evolutionary information [57,74]. Several methods have performed close prediction accuracies by using neural network based methods and profile scores [23, 27, 44, 59, 72, 75, 79].

A new alignment search method has been introduced which automatically aligns protein families based on profiles. Several research groups have developed the profile-based databases searches [25, 29, 33, 42, 51, 64, 85]. The development of PSI-BLAST and Hidden Markov Models have been increased the prediction performances [1, 41]. David Jones pioneered the use of the iterated PSI-BLAST searches on large databases automatically. He has developed the PSIPRED secondary structure method using that PSI-BLAST searches results [39]. Kevin Karplus et al. have proposed their own method (SAM-T99sec) which finds the diverged profiles using Hidden Markov Models [42]. Cuff and Barton also used PSI-BLAST alignments for JPred2 [21]. SSpro used a different architecture which was an advanced recursive neural network system [3]. This method has tried to solve the problem of predicting too short segments by using the recursive neural network and multiple alignments.

The current state of the art for the secondary structure prediction is near 78% for three state per residue accuracy (the percentage of α-helices, β-sheets, and coils). The methods PROF, PSIPRED, and SSpro perform the most accurate performances, according to EVA results, an automatic server evaluating the automatic prediction servers [3,39,76,77]. EVA takes the newest experimental structures added to PDB, sends the sequences to all prediction servers, and collects the results [5].

The existing methods improve the prediction of the α-helix and β-strand secondary structure elements. There exist small stable structures such as turns, hairpin loops. However, the prediction of these structures is not so easy and the research in this area are not satisfactory.

After this short review of the secondary structure prediction methods, we want to mention about the scope of the thesis. We have worked on the small secondary structures, β-**turns**, which have a critical role on the folding of protein. The formation of these turns has been thought to be an important early step in the protein folding pathway. The identification of β-turns would provide important advancements for the protein folding pathway; since, β-turns are commonly found to link

two strands of anti-parallel beta-sheet. We have developed **Hidden Markov Models** to identify the location of β-turns in a given protein sequence. Type of β-turns has been also identified by **Artificial Neural Networks**.

Some third generation structure prediction approaches have tried to improve the accuracy of assigning the secondary structural class (all-α, all-β, α/β, other). In another part of the thesis, we have applied **Support Vector Machines** to improve the classification accuracy of the secondary structural class of proteins.

1.3   Organization of The Thesis

In Chapter 2, we present our work for the classification of the protein structural classes by Support Vector Machines. In Chapter 3, the work on predicting of the location of β-turns by Hidden Markov Models is presented. Finally in Chapter 4, we present the classification of type of β-turns by Artificial Neural Networks.

Chapter 2

Protein Structural Class Determination Using Support Vector Machines

2.1 Introduction

The term **structural class** was introduced by Levitt and Chothia [52, 71]; they classified proteins into four structural classes according to their secondary structure contents: all-α, all-β, α/β, $\alpha+\beta$ (see Figure 2.1). These four structural classes are described in below:

- Class α contains several α-helices connected by loops.

- Class β contains antiparallel β-sheets, generally two sheets are in close contacts to form sandwich shape.

- Class α/β contains parallel β-sheets with intervening α-helices. Parallel β-strands might form into a barrel structure that is surrounded by α-helices.

- Class $\alpha+\beta$ contains separated α-helices and antiparallel β-sheets.

Whereas these four structural classes are used in the SCOP hierarchy, because of their similarity, the classes α/β and $\alpha+\beta$ are combined into the α-β class in the CATH hierarchy [62, 67].

The structural class information provides a rough description of a protein's 3D structure by giving evolutionary relationships between proteins; since, the structural classes are on the top of the protein classification hierarchy and each class includes
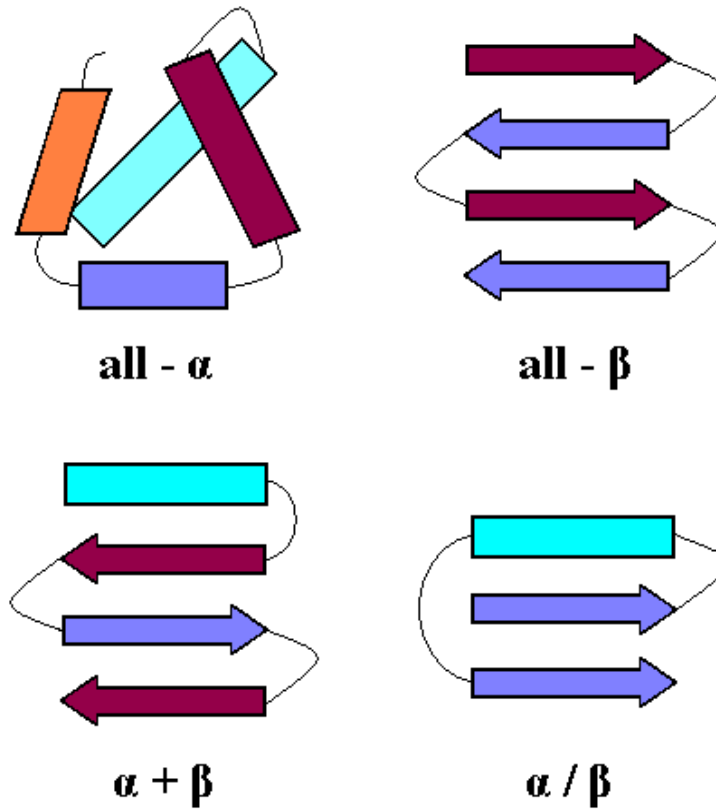
Figure 2.1: The illustration of main four structural classes.

several different folds, superfamilies, and families. Hence, we could obtain useful information about a protein by finding its structural class. If we have a protein whose structural class is known, we could reduce the search space of the structure prediction problem. For instance, the structural class information has been used in some secondary structure prediction algorithms [22, 26, 46].

The **fold** refers to the combination of the secondary structures in 3D conformation. The proteins with same fold have the same combination of the secondary structures. A protein **family** is composed of homolog proteins with the same function in both same or different organisms. In families, some proteins share a significant sequence similarity but some of them are not. When a couple of protein families that have distant evolutionary relations come together, they form a protein **superfamily**. Superfamily proteins share common structural features; however, there can be variation on the arrangement and number of secondary structures.

2.2 Previous Work

During the past ten years, many scientists worked on the structural classification problem [2,9,10,12,14,17,19,24,45,60,63,95]. The classification methods are various: the Component Coupled Algorithm (CCA), Artificial Neural Networks, Support Vector Machines (SVM) etc. However, they typically use the simple feature of amino acid composition of the protein as the base for the classification.

Among these structural classification studies, an independently developed work uses a SVM as the classification tool and the amino acid composition [10]. Although their data set is completely different, the classification tool and feature is similar with our method. Their average classification performance in the Jackknife test is 93.2%, for 204 protein domains.

Another method, the CCA, also using the amino acid composition, had reported very successful results for the same problem. So, we wanted to duplicate and improve this work, in our study. The details of the CCA is explained in the following section.

2.2.1 Component Coupled Algorithm

K.C. Chou used what they called the **Component Coupled Algorithm** to assign a protein into one of the four structural classes [14]. The CCA is more sophisticated from the earlier techniques since, it uses the Mahalanobis distance [55] as its discriminant function, taking into effect the covariance of amino acid compositions (coupling), in addition to only considering the mean amino acid composition vectors of structural classes for the classification. The brief summary of CCA is given below:

The **Amino Acid Composition** (AAC) represents protein with a 20 dimensional vector corresponding to the composition (frequency of occurrence) of the 20 amino acids in the protein. Since, the frequencies sum up to 1, only 19 out of 20 are independent and the AAC can be represented in 19 independent dimensions. The AAC vector of a protein is:

$$X = \begin{bmatrix} x_1 \\ x_2 \\ \vdots \\ x_{19} \end{bmatrix} \qquad (2.1)$$

where x_k is the occurrence frequency of the kth amino acid.

Assuming normally distributed classes, the distance of a given protein P to a particular class ϕ can be calculated using the Mahalanobis distance in a way to take into account the spread of the class as:

$$D(P, X^\phi) = (P - X^\phi)^T C_\phi^{-1} (P - X^\phi) \qquad (2.2)$$

where X^ϕ is the mean AAC vector over all the proteins in the structural class ϕ and C_ϕ^{-1} is the inverse of the covariance matrix C_ϕ of that class. The covariance matrix of a given structural class ϕ captures the covariance of the AAC vectors within that class as:

$$C_\phi = \begin{bmatrix} c_{1,1}^\phi & c_{1,2}^\phi & \cdots & c_{1,19}^\phi \\ c_{2,2}^\phi & c_{2,2}^\phi & \cdots & c_{2,19}^\phi \\ \vdots & \vdots & \ddots & \vdots \\ c_{19,1}^\phi & c_{19,2}^\phi & \cdots & c_{19,19}^\phi \end{bmatrix} \qquad (2.3)$$

where each $c_{i,j}^\phi$ element is given by:

$$c_{i,j}^\phi = \sum_{k=1}^{N_\phi} [x_{k,i}^\phi - X_i^\phi][x_{k,j}^\phi - X_j^\phi] \qquad (2.4)$$

The classification of protein P into one of the structural classes is done by choosing the class X with the smallest distance as:

$$D(P, X^\xi) = Min(D(P, X^\alpha), D(P, X^\beta), D(P, X^{\alpha/\beta}), D(P, X^{\alpha+\beta})) \qquad (2.5)$$

where ξ is the structural class (the winner) which has the least Mahalanobis distance to the vector P.

2.3 Our Method

Although the AAC largely determines structural class, its capacity is limited, since one looses information by representing a protein with only a 20 dimensional vector. Therefore, we try to improve the classification capacity of the AAC by extending it to the **Trio Amino Acid Composition** (Trio AAC). The Trio AAC is calculated from the occurrence frequencies of consecutive amino acid triplets in a protein.

The frequency distribution of neighboring triplets is very sparse because of the high dimensionality of the Trio AAC input vector (20^3). Furthermore, one also has to take into account the evolutionary information which shows that certain amino acids can be replaced by the others without disrupting the function of a protein. These replacements generally occur between amino acids which have similar physical and chemical properties. Hence, several different clustering of the amino acids which take into account these similarities and reduce the dimensionality, have been used [87].

In this thesis, the performance of SVMs and the CCA using the AAC feature (described in the previous Section 2.2.1), are compared to observe their classification capability. The CCA is applied on the same data set to classify the protein using the Mahalanobis distance between its AAC vector and each structural class. Both the AAC and the Trio AAC features have been used on SVMs. The detailed explanation of the construction of the feature sets will be given in Section 2.3.3.

2.3.1 Support Vector Machine

SVM (see Appendix A) is a supervised machine learning technique which seeks an optimal discrimination of two classes, in high dimensional feature space. The superior generalization power, especially for high dimensional data, and fast convergence during training are the main advantages of SVMs. We also preferred to use SVMs as the classification tool because of its high classification performance on the protein structural classification problem [10, 24, 88]. The LIBSVM software have been applied in predicting the structural classes [13].

Generally, SVMs are designed for 2-class classification problems whereas our work requires a multi-class classification. Multi-class classification is typically solved

using voting schemes based on combining binary classification decision functions. In the LIBSVM tool that we have used, the **one-against-one** approach is used. In this scheme, $k(k-1)/2$ classifiers are constructed for k class, each one trained with data from only two different classes. To obtain the multi-class label for a given data point, each of these classifiers makes its decision and the class label with the maximum number of votes overall is designated as the correct label of a data point.

In order to get good classification results the parameters of SVM, especially the kernel type and the error-margin tradeoff (C), should be fixed. The Gaussian kernels are used since they typically provide better linear separation compared to Polynomial and Sigmoid kernels. The value of the parameter C was fixed during the training and later used during the testing. The best performance was obtained with C values ranging from 10 to 100 in various tasks.

2.3.2   Data Set

We have used the same data set with Chou to make the comparison between the performances of classification methods [14]. Data set consist of 117 training proteins and 63 test proteins. Since we could not find the PDB files of 4 proteins (1CTC, 1LIG, 1PRF in training set; 1PDE in test set) included in their database, we used a total of 117+63 proteins instead of 120+64 [5]. The total number of proteins for each class are listed in Table 2.1.

The PDB files are used to form both the AAC and the Trio AAC vectors for the given proteins. After collecting the PDB files of proteins, we extract the amino acid sequence of each one. The amino acid sequences are then converted to the feature vectors as described in Section 2.3.3.

Class ID	Training	Test
all-α	29	8
all-β	30	22
α/β	29	9
$\alpha+\beta$	29	24
Total:	117	63

Table 2.1: The total number of proteins in each structural class.

There are several strategies to classify a protein into one of the structural classes. It is commonly based on the percentage of α-helix and β-sheet residues in the protein. K.C. Chou also uses the same method to classify proteins in the data set. The percentage of α-helix and β-sheet residues for each class is explained below:

- All-α : α-helix $> 40\%$ and β-sheet $< 5\%$

- All-β : α-helix $< 5\%$ and β-sheet $> 40\%$

- α/β : α-helix $> 15\%$ and β-sheet $> 15\%$ and more than 60% parallel β-sheets

- $\alpha+\beta$: α-helix $> 15\%$ and β-sheet $> 15\%$ and more than 60% antiparallel β-sheets

2.3.3 Feature Sets

The training and test data obtained from the PDB are used to form feature sets. The amino acid sequences are converted to the feature vectors as explained below.

AAC

The AAC represents protein with a 20 dimensional vector corresponding to the composition (frequency of occurrence) of the 20 amino acids in the protein. The AAC can be used as a 19 dimensional vector since the frequencies sum up to 1, only 19 out of 20 amino acids are independent; hence, only 19 dimensions of the AAC vector is used as input. The details of constructing AAC vector was given in previous Section 2.2.1.

Trio AAC

The Trio AAC is the occurrence frequency of all possible consecutive triplets of amino acids, or **amino acid clusters**, in the protein. Whereas the AAC is a 20-dimensional vector, the neighborhood composition of triplets of amino acids requires a 20x20x20 (8000) dimensional vector (e.g. AAA, AAC, ...). We reduce the dimensionality of the Trio AAC input vector using various different clusterings of the amino acids, also taking into account the evolutionary information.

The amino acid clusters are constructed according to hydrophobicity and charge information of amino acids [87]. We experimented with different # of clusters: 5, 9, or 14 clusters of the amino acids, giving Trio AAC vectors of 125 (5^3), 729 (9^3), and 2744 (14^3) dimensions, respectively. The content of each amino acid cluster, for the case of 9 groups, is shown in Table 2.2.

Cluster ID	Amino acid name
1	V I L M F
2	W Y
3	A
4	E D
5	R K
6	G
7	S T N Q H
8	C
9	P

Table 2.2: The content of each amino acid cluster for the 9 cluster case.

2.4   Results and Discussion

In order to classify a protein into one of the four structural classes (all-α, all-β, α/β, $\alpha+\beta$), several approaches have been studied. We first tried to duplicate the previous work of K.C. Chou, called Component Coupled Algorithm, which reports a 95% performance on classifying proteins [14]. Due to such a high performance, Wang and Yuan previously tried to replicate this work, as well [92]. Although we used the same algorithm and data set, our effort to replicate their experiment was unsuccessful, as was the case for Wang and Yuan.

After applying the CCA, a different classification technique, SVM (as described in 2.3.1), is used with the feature sets of AAC and Trio AAC which incorporates evolutionary and neighborhood information to the AAC.

In summary, we have measured the performance of three algorithms: CCA, SVM with the AAC feature, and SVM with the Trio AAC feature. The performance of each of these approaches is analyzed in terms of their:

- performance of learning the training data (train and test with training data)

- generalization performance on test data (train with training data, test with test data)

- generalization performance using cross-validation techniques (train with all data, test with the one left out)

2.4.1 Training Performance

The term **training performance** is used to denote the level of learning after training; previously the term **self-consistency** was used to refer to the same concept. Specifically, the training performance is the percentage of the correctly classified training data, once the training completes. Hence, it is an indication of how well the training data is learned. Even though, the performance result on the test set is the relevant factor, as it indicates the success on unseen data, the training performance is also useful because it indicates how well the problem is learnt using the particular classification method.

The training performance of our CCA and SVM are summarized on Table 2.3, along with Chou's reported results [14]. Neither the SVM nor the CCA could achieve 100% training performance. The data points may not be linearly separable in the feature space, due to the mapping done by the kernel function. Hence, the training performance with less than 100% is probable for the SVM.

Class Name	Chou's Result	CCA	SVM^{AAC}	$SVM^{TrioAAC}$
all-α	100%	100%	100%	100%
all-β	100%	100%	96.6%	96.6%
α/β	96.7%	82.7%	100%	100%
$\alpha+\beta$	100%	96.5%	100%	100%
Average	99.1%	94.8%	99.1%	99.1%

Table 2.3: *Training performances* of Chou [14] versus our results using CCA and SVM, using the AAC or the Trio AAC.

2.4.2 Test Performance

Table 2.4 summarizes the test performance of the algorithms on the test set (63 proteins), after being trained on the training set (117 proteins). The AAC is used as feature vector for both CCA and SVM. The Trio AAC is also applied as the input to the SVM.

The average test performance of the SVM using the AAC is almost the same with the CCA (see Table 2.4). The performance of the SVM with Trio AAC feature was found to be lower compared to the AAC feature. The reason for the lower performance of the Trio AAC might be the high dimensionality of the input data, compared to the size of the training set: if some data points in test set are not represented in the training set, the SVM could not classify these test data properly. Hence, the Trio AAC vector might be sparse and insufficient to represent the structural class $\alpha+\beta$ especially, due to the high dimensionality.

Class Name	CCA	SVM^{AAC}	$SVM^{TrioAAC}$
all-α	62.5%	62.5%	62.5%
all-β	77.2%	77.2%	81.8%
α/β	66.6%	100%	77.7%
$\alpha+\beta$	75.0%	58.3%	25.0%
Average	73.0%	71.4%	57.1%

Table 2.4: Test performances of classifiers with training performances shown in Table 2.3. The AAC is applied in both method the CCA and the SVM, in addition the Trio AAC is used for the SVM.

2.4.3 Test Performance using the Jackknife Method

The **Jackknife test**, also called the leave-one-out test, is a cross-validation technique which was invented in order to use all the available data for training, while still obtaining an unbiased test. In the Jackknife test, we train with all the data (train + test) leaving one sample out each time; then we test with that one sample, on that round of train-test cycle. This method uses all of the data for testing; but since the test data is not used for the corresponding training phase, the testing is unbiased.

Table 2.5 displays the results obtained in experiments using the SVM in con-

junction with the AAC or the Trio AAC. According to the first Jackknife test results, the performance of the SVM is quite successful. The average classification rates are 85% and 92.7% for the AAC and the Trio AAC, respectively. We achieved the 92.7% classification rate using the Trio AAC which is constructed using 9 amino acid clusters. The high classification performance shows that the combination of a powerful tool, SVM, and a representative feature set, the Trio AAC, could improve the classification accuracy.

Class Name	SVM^{AAC}		$SVM^{TrioAAC}$	
	%	#	%	#
all-α	72.9%	(27/37)	72.9%	(27/37)
all-β	100%	(52/52)	98%	(51/52)
α/β	84.2%	(32/38)	94.7%	(36/38)
$\alpha+\beta$	79.2%	(42/53)	100%	(53/53)
Average	85.0%	(153/180)	92.7%	(167/180)

Table 2.5: Jackknife test performance of the SVM on (117+63) proteins, using the AAC or the Trio AAC.

Another Jackknife test has been performed on 117 training proteins in order to compare our results to the previous work of Wang and Yuan [92]. They also try to duplicate Chou's work using the CCA and the AAC feature. The results for both algorithms, CCA and SVM, are shown in Table 2.6. According to the second Jackknife test results, the average classification rate of the SVM (using the AAC) is more than 20% higher than CCA performance. Hence, we say that SVM is more successful classification method than CCA. The average classification rate is 84.6% using the Trio AAC, as shown in Table 2.6. The Trio AAC proved its better classification ability one more time.

Class Name	CCA	SVM^{AAC}	$SVM^{TrioAAC}$
all-α	66.7%	75.8%	82.7%
all-β	56.7%	93.3%	93.3%
α/β	43.3%	75.0%	92.8%
$\alpha+\beta$	46.7%	55.1%	72.4%
Average	53.3%	74.3%	84.6%

Table 2.6: Jackknife test performance on 117 proteins (the training set only), as done by Wang and Yuan (CCA) [92] and our results, obtained by SVM method using the AAC or the Trio AAC.

2.4.4 Discussion

The SVM could perform a better classification using more data for each structural class; since, the average classification results for the first Jackknife test (Table 2.5) is 8-10% better than the results for the second Jackknife test (Table 2.6).

The comparison of two the input vectors, AAC and Trio AAC, shows that the Trio AAC provides, on the average, 8-10% improvement on the classification performance. We experimented with different # of clusters: 5, 9, and 14 clusters of the amino acids, giving Trio AAC vectors. The experiment with 9 clusters of the amino acids has the highest classification rates (Table 2.5, 2.6). The better performance of the Trio AAC proves the original assumption that the neighborhood and evolutionary information positively contributes on the classification accuracy.

According to our test results, the average generalization performance of CCA is near 73% (Table 2.4). However, we could not achieve the 95% classification rate of Chou work [14]. On the other hand, the SVM performance is higher than the CCA according to Jackknife test results (Table 2.5, 2.6). The classification performance of SVM is also improved by using the Trio AAC representation. We used several different amino acid clusters and the clustering into 9 groups (Table 2.2) gave the best performance.

2.5 Summary and Conclusion

Several scientists have attempted to solve the protein structural classification problem using different classification tools and feature sets. We have compared both the SVM and the CCA with AAC feature to observe their classification capability. Besides, the ability of the Trio AAC feature in the structural classification problem has been measured.

In literature, there are two studies which use the similar feature vectors with the Trio AAC. These studies are working on the remote homology detection problem by using the SVM and the amino acid neighboring effect [50,90]. Although their feature vector seems to be similar with the Trio AAC vector, the idea of using amino acid clusters (to gather the analogous amino acids into one group) for the Trio AAC has

not been applied. The implementation of the kernel function is also different from our kernel functions. Their claim is that the computational complexity is minimized by making the calculations using a new kernel which is called the string or spectrum kernel. However, we preferred using one (Gaussian) of the common kernel functions of SVMs.

The research of Cai et.al. might be comparable to our work; since they use SVMs and the AAC [10]. The average classification performance of their work in the Jackknife test is 93.2% for 204 protein domains. Although we have worked on completely different data set, our average classification performance is 92.7% for the Jackknife test on entire data set using the Trio AAC feature (Table 2.5).

In conclusion, the utilization of a feature vector which includes neighborhood information and grouping of the amino acids provides a significant increase on the protein structural classification capacity of SVMs.

Chapter 3

The Prediction of The Location of β-Turns by Hidden Markov Models

3.1   Introduction

Several different methods have been developed to predict the α-helix and β-sheet regions of a protein. However, there exist other secondary structure types: turns, hairpins, bulges, and loops. Even though the β-turns are also important in the folding of a protein, the amount of research to identify β-turns is very limited compared to the amount of research on the prediction of α-helices and β-sheets. We work on the prediction of the β-turn regions using Hidden Markov Models (HMM) since, HMMs have proven to be very successful in similar problems, such as speech recognition, where the input also displays a sequential and stochastic nature.

Figure 3.1: A turn structure between two anti-parallel β-sheets.

The present secondary structure prediction methods give the results in terms of the helix, sheet, and coil region. According to the definition of present methods: turns, hairpins, bulges, and loops are recognized in the coil region. However, the

combination of all these secondary structures constructs the 3D structure of proteins and the prediction of each secondary structure would provide a positive contribution for the prediction of 3D structure. For instance, β-turns change the direction of the protein chain; so they have a significant function during the folding pathway. Figure 3.1 shows a turn structure between two anti-parallel β-sheets. The development of an accurate method for identifying the location of β-turns within a protein sequence would aid the identification of other structural motifs (e.g. β-hairpins).

3.2   Overview of β-Turns

Tight turn structures are the most common type of non-repetitive structures in proteins [40]. Tight turns are classified according to their length: δ-turn, γ-turn, β-turn, α-turn, π-turn which involve 2, 3, 4, 5, and 6 amino acids, respectively. Tight turns can provide a direction change for the polypeptide chain (see Figure 3.1 and 3.2). They reside on the surface of the protein and interact with other proteins.

Among tight turns, β-turns are the most common ones, formed by four consecutive residues (R_i, R_{i+1}, R_{i+2}, R_{i+3}). The β-turns comprise on the average 25% of the residues in proteins [40]. There are conflict definitions of the β-turns in literature. Venkatachalam first identified categories of turns while studying favorable conformations of short peptides [89]. Richardson defined turns on the basis of ϕ, ψ angles and defined six distinct categories, and one miscellaneous category (type IV turn) [70]. Lewis et.al., found that 25% of turns do not contain the hydrogen bond as was proposed by Venkatachalam. They proposed that a β-turn also involves non-helical main chain angles ϕ and ψ [53]. After that β-turns have been classified into nine different types (I, I', II, II', VIa1, VIa2, VIb, IV, VIII) based on dihedral angles of the inner residues at i+1 and i+2 positions [34, 70, 89]. These nine types of β-turns are also used in this study.

The most common definition for β-turns is that they are comprised of four consecutive residues where the distance between $C\alpha_i$ and $C\alpha_{i+3}$ is less than $7\mathring{A}$ and tetrapeptide chain is not in a helical conformation [70, 73]. We also use this definition of the β-turns in this study.
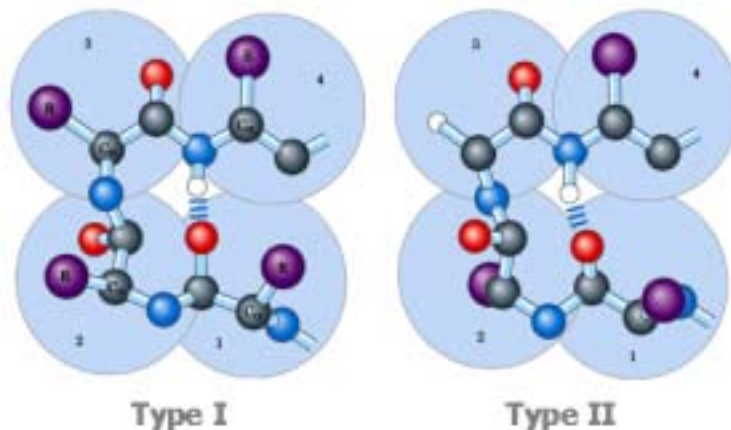
Figure 3.2: β-turns consist of four residues which are marked by the blue circles. The C_α atoms are shown in grey. The hydrogen bond exists between residue i (CO-red atom) and residue i+3 (NH-blue atom). Two types of β-turns are very common, type I and type II [49]. Note that the difference between the angles in the backbone of the second and third residues. This angle is one criteria to determine type of β-turns.

3.3 Previous Work

Most of the β-turn prediction approaches are statistical and based on the positional information of the amino acids. They calculate the propensity of each amino acid at the i and i+3 positions of a β-turn.

The Chou-Fasman algorithm is based on calculating the product of amino acid probabilities at each of the four positions in a β-turn [18]. In other words, the likelihood of a four amino acid sequence to be a β-turn is computed as the product of the likelihoods of the amino acids being at the through it four locations of a β-turn. The conformational parameters for each amino acid are calculated by considering the relative frequency of a given amino acid within a protein (the occurrence of each amino acid in a β-turn and the fraction of all residues occurring in a β-turn).

The conformational potentials, positional potentials and turn type dependent positional potentials of each amino acid are recalculated by Thornton [93]. Chou proposed a new model which is called **1-4 & 2-3 correlation model** where he takes into consideration the coupling effect between the first and fourth residues, and between the second and third residues in β-turns [94]. Chou proposed another model, **sequence coupled model** which is based on first-order Markov chains and involves conditional probabilities at each position [15].

The milestone for the β-turn prediction approaches was to apply one of the machine learning techniques, Artificial Neural Networks; since they provided the improvement on the prediction accuracy. Firstly, McGregor et.al., proposed a method to predict β-turns by a multilayer neural network [58].

The second neural network based approach was the BTPRED [82]. A feedforward neural network with one hidden layer is used to predict whether a given residue is part of a β-turn or not. Their data set includes 300 non-homologous proteins; but, it is smaller than our data set. The input vector of the network is formed using binary encoding where each amino acid is represented by a single one and 19 zeros. It also used secondary structure information obtained from PHDsec program [74]. The percentage of the correctly predicted β-turns ($Q_{observed}$) and Matthews Correlation Coefficient (MCC) value are 31% and 0.35, respectively.

BetaTPred2 is the last one that uses two feedforward neural networks and a larger data set including 426 non-homologous proteins [43]. The first network has one hidden layer and is trained using multiple sequence alignments in the PSI-BLAST form [1]. The second network is trained by the initial prediction of the first network and PSIPRED secondary structure information [39]. They provide a significant improvement on the performance by giving the evolutionary information with PSI-BLAST multiple alignments. The percentage of the correctly predicted β-turns and MCC value are 72% and 0.43, respectively.

In the literature, we have not found work using HMMs to determine the location of β-turns in the given protein sequence. In addition, the sequence of the β-turns displays the sequential and stochastic nature of HMMs. Hence, the reasons of using HMMs for the prediction of the β-turns are the lack of usage of HMMs on this problem and the suitable nature of HMMs.

3.4   HMMs for β-Turn Prediction

HMM is a statistical model of sequential data commonly used in machine learning applications, such as speech and writing recognition, as well as secondary structure prediction. HMMs are good at capturing the temporal nature of a process and they

are well suited for problems with a simple grammatical structure.

HMM is a generative model consisting of a hidden Markov chain of states and a series of observations generated by each state. It can capture the information of a set of sequences and capable of outputting sequences according to the information. Whereas in a Markov chain, the probability of observation (x_i) only dependent on previous observation (x_{i-1}) but not on observations further before $(x_{i-2}, \cdots, x_i)$.

In classification tasks, we want to estimate $P(M|O)$, the probability of a model (M) for a given observation sequence (O). For instance, in a β-turn prediction problem, we want to find the most likely secondary structure of a given amino acid subsequence. HMMs can estimate the likelihood of a given observation to be generated by a particular model, $P(O|M)$. These probabilities, $P(M|O)$ and $P(O|M)$, are combined via Bayes' theorem as follows :

$$P(M|O) = \frac{P(O|M)\ P(M)}{P(O)} \tag{3.1}$$

where P(O) is the unconditional probability and it is the same for all models; P(M) is the prior probability of a model (e.g. the probability of being an α-helix structure). $P(O|M)$ is estimated via the forward algorithm

In an HMM, the states are hidden. The Viterbi Algorithm finds the most likely path (state sequence) of a given training data. The most probable secondary structure information (β-turn, α-helix, β-sheet, coil) of a given sequence can be predicted by applying the Viterbi decoding.

Training sequences are used to estimate the model, the state transition and the emission, probabilities and test sequences are used to evaluate the model. The model estimation is done by the Baum-Welch algorithm which is an iterative algorithm that maximizes the likelihood of the training sequences. The large review of HMMs is given in Appendix B.

3.4.1 The Topology of Our HMMs

The aim is to predict β-turn from given amino acid sequence. We train the HMMs not only with the β-turn words, but also other secondary structure elements (α-helix, β-sheet, coil) to able to introduce the neighborhood information between the secondary structures. Therefore, four different words are used to define an HMM: **T, H, B,** and **C** stand for β-turn, α-helix, β-sheet, and coil, respectively.

Three different HMM architectures have been designed:

- **Simple Model**: It consists of four basic HMMs which are called T, H, B, and C models. Each model stands for a secondary structure element and includes four or five states. The entire system is built up of four basic model and each one is connected to other. This a simple model is used to determine the base success of HMMs in β-turn prediction problem. Figure 3.3 illustrates the relations between four simple HMMs.
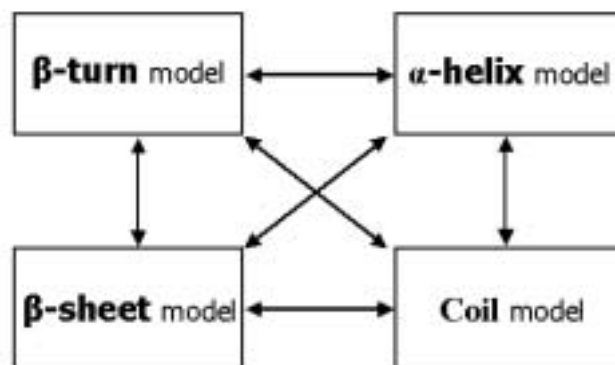
Figure 3.3: The relations between four simple HMMs. The directional arrow indicates a transition for two sides.

- **Triplet-word Model**: It is built up using the triplet of the simple models (e.g. THB, TBC, HCB, THT, etc). The start and end position of the each protein sequence is marked by the **X** word; so, there are such triplets: XTH, XTB, TCX, HBX, etc. The one restriction is that the repetition of the same word is not allowed in consecutive words e.g. TTB, CBB, HHT, CCB, etc. Each triplet model consists of four or five states and the word repetition should be done in these states. The middle word of a triplet represents the actual processing

model. In other words, the first word of a triplet represents the previous model and the third one represents the next model. Hence, neighborhood relations (e.g. some β-strand are followed by a β-turn) can be introduced using the trio combinations of the simple models. Figure 3.4 explains the topology and construction phases of a triplet-word model. In total, there are 60 different HMMs for the triplet-word model.
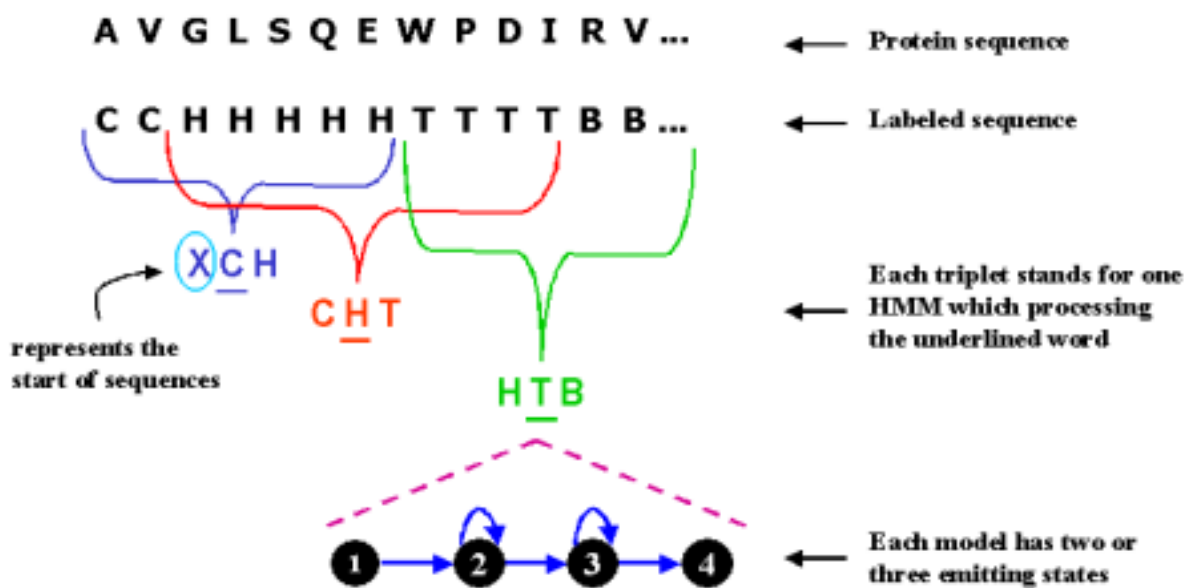
Figure 3.4: The illustration of constructing steps of a triplet-word model.

- **Complex Model**: The topology of the complex model is different from the previous models. Each model consists of four consecutive words (T, H, B, or C) not models. The reason for using the window with four words is to introduce the β-turn context more precisely since the β-turns consist of four residues. Furthermore, the sliding window method is used to capture multiple β-turns which follow consecutively another β-turns.

The first word in the complex model is the actual processing word by this model. In addition, the complex models include three states. Although in the previous models have two or three emitting states, a complex models have just one emitting state. The end point of the protein sequence is marked by **X** word. There are 95 different HMMs for the complex model. The total number of complex models should be much higher when considering all possible

32

combinations of four words. However, there are some restrictions due to the secondary structure formation rules. The crucial restriction is that an α-helix and a β-sheet consist of at least four and two residues, respectively. Figure 3.5 explains the topology and construction phases of a complex model.
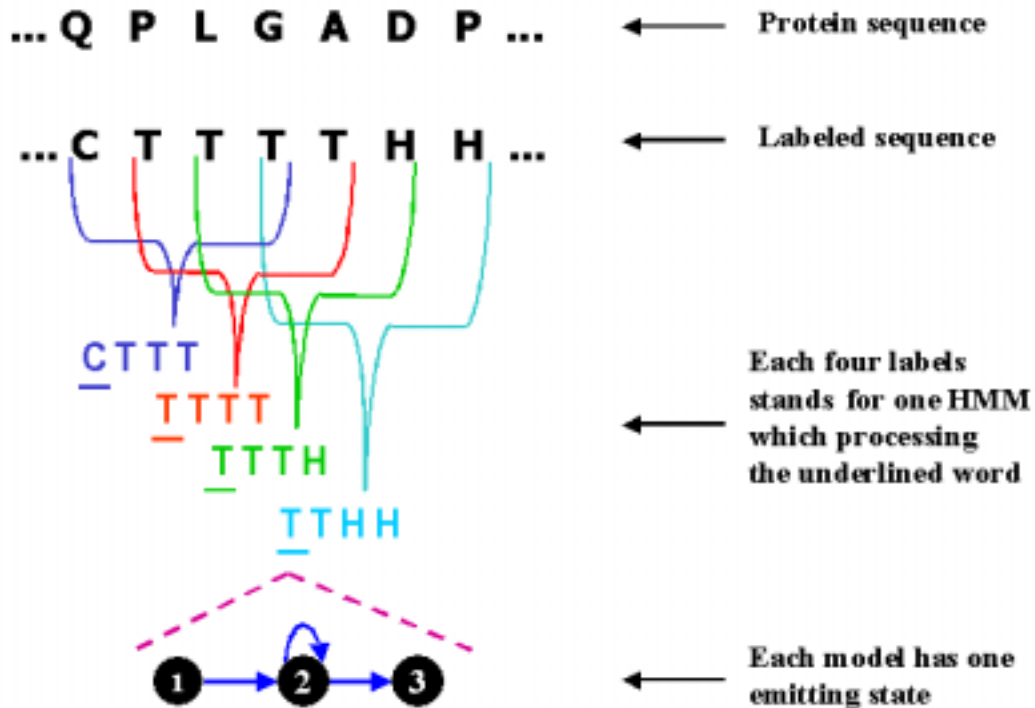
Figure 3.5: The illustration of constructing steps of a complex model.

One can represent the amino acids in 1-of-n representation, using 20 inputs where the input corresponding to the amino acid is set to 1 while all others are set to 0. We prefer to represent the amino acids by their 3D similarity scores instead of giving 1-of-n representation for each amino acid. The first reason of using a 3D similarity score is to give the evolutionary (similarity) information between amino acids. The second one is that HTK tool is designed for the speech recognition and the tool becomes more successful by training with continuous data. The details of how we construct the amino acid similarity score will be described in Section 3.4.3.

The definition of an HMM must specify the model topology, the transition parameters and the output distribution parameters. Our HMM definition includes four or five states for systems. Each state j has an associated observation probability distribution $b_j(O_t)$ which represents the probability of generating observation O_t at

time t. Each pair of states i and j has an associated transition probability a_{ij} . The entry state and the exit state are non-emitting states.

Figure 3.6 shows a simple left to right HMM with four states. Two of these are emitting states and have output probability distributions associated with them. The start and end states have no emission probabilities. The transition matrix for this model will have four rows and four columns. Each row's probability will sum to one except for the final row which is always all zero since no transitions are allowed out of the final state. HTK is principally concerned with continuous density models in which each observation probability distribution is represented by a mixture of Gaussian density.
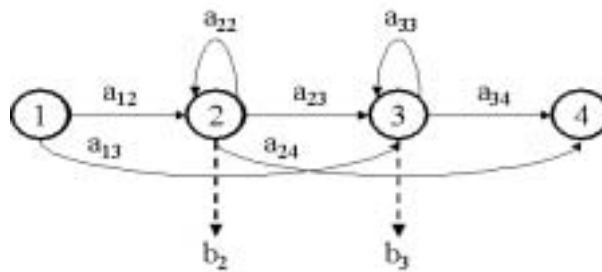
Figure 3.6: Simple left to right HMM with four states.

3.4.2 Data Set

The representative protein dataset for our analysis was obtained from the Protein Data Bank using the program PDB_SELECT [5, 30]. The dataset is available under the filename "recent.pdb_select" (dated 22 December 2002) on the ftp site [28]. The representative protein chains were selected so that no two chains had more than 25% sequence identity. Protein chains determined by X-ray crystallography at 2Å resolution or less, containing at least one β-turn, were used in the analysis. Data set consists of 1190 training and 163 test protein chains.

The PROMOTIF program which provides details of the location and types of structural motifs in proteins of known three dimensional structure in the PDB, is used to extract the β-turns classified into the nine known types (I, II, I', II', VIa1, VIa2, VIb, IV, VIII) [35].

In order to make the labeling of protein sequences, each amino acid is marked by its secondary structure content: T, H, B, or C. We collected all the label files into one file which is called the **master label file**. Another operation is to construct the main data files whose representation is very similar to the manipulated speech waveforms. Each amino acid is replaced with its similarity score as explained in Section 3.4.3. Then we took a window with seven length (the total number of amino acids) and processed each protein sequence from start to end using seven residues window.

3.4.3 Feature Set

Amino Acid Similarity Score

In this study, an amino acid similarity matrix is used due to containing evolutionary information between proteins and similarity between amino acids. The amino acid similarity matrix is constructed by converting the protein similarity matrices (e.g., PAM, Blossom, etc.).

The protein similarity matrices are constructed by considering the evolutionary relationships between proteins. During the evolution, some amino acids can be replaced by other amino acids; so, the protein similarity matrices give the probabilities of changing from one amino acid to another. Such a similarity matrix provides the evolutionary and similarity information about the amino acids.

We use the PAM250 similarity matrix which is 20D matrix which captures the principal physicochemical properties of the amino acids. The PAM250 matrix is reduced into a 3D vector since we could represent the same amino acid properties in 3D environment [36]. The dimension reduction is done by a function mapping; it was performed by a simple neural network that has 1 hidden layer and 3 hidden neurons. The 20D similarity matrix is given as the input, the output is the 3D vector for each amino acid. The 3D output vector for each amino acid is given in Table 3.1.

Amino Acid	x	y	z
C	34.4	30.5	18.8
G	34.4	30.7	18.7
P	34.3	30.6	18.7
S	34.2	30.4	18.7
A	34.3	30.5	18.7
T	34.2	30.5	18.7
D	34.3	30.7	18.7
E	34.3	30.7	18.6
N	34.2	30.5	18.6
Q	34.2	30.6	18.6
H	34.1	30.4	18.6
K	34.1	30.5	18.6
R	34.1	30.5	18.6
V	34.2	30.4	18.6
M	34.1	30.4	18.6
I	34.0	30.3	18.6
L	34.0	30.3	18.6
F	34.0	30.1	18.6
Y	34.0	30.2	18.6
W	33.7	30.0	18.5

Table 3.1: The similarity score of each amino acid in 3D.

3.5 Results and Discussion

Several different HMMs are developed and the model parameters are estimated using protein training data. Then the recognition performance should be monitored on testing data. In the next sections, the performance measures and recognition results will be explained in detail.

3.5.1 Performance Measures

There are several different statistical measures to determine the prediction performances. We have used four different parameters to measure the performance of our HMMs as described by Shepherd et.al. [82]. Some necessary definitions used in these parameters are as follows:

c_t : the number of correctly classified β-turn residues

c_o : the number of correctly classified non-β-turn residues

t : the total number of residues in a protein

e_o : the number of non-β-turn residues incorrectly classified as β-turn residues

e_t : the number of β-turn residues incorrectly classified as non-β-turn residues

The prediction performance of the HMMs is expressed by four parameters:

1. Q_{total} is the percentage of correctly classified residues given as:

$$Q_{total} = \left(\frac{c_t + c_o}{t} \right) 100 \tag{3.2}$$

Q_{total} is also known as **prediction accuracy**; it is the percentage of correct prediction. This measure does not take into account disparities in the number of β-turns and non-turns: there is a risk of losing the information because of the dominance of non-turn residues.

2. Matthews Correlation Coefficient (MCC) is defined as:

$$MCC = \frac{c_t c_o - e_o e_t}{\sqrt{(c_t + e_o)(c_t + e_o)(c_o + e_t)(c_o + e_t)}} \tag{3.3}$$

MCC solves the disparity problem seems in Q_{total} measure. It is a measure that accounts for both over and under predictions.

3. $Q_{predicted}$ is defined as:

$$Q_{predicted} = \left(\frac{c_t}{c_t + e_o} \right) 100 \tag{3.4}$$

It is the percentage of β-turn predictions that are correct. It is also called **specificity**, the proportion of true negatives.

4. $Q_{observed}$ is defined as:

$$Q_{observed} = \left(\frac{c_t}{c_t + e_t} \right) 100 \tag{3.5}$$

It is the percentage of observed β-turns that are correctly predicted. It is also called **sensitivity**, the proportion of true positives.

3.5.2 Recognition Performance

The left to right HMMs are used to predict the location of β-turns in a given protein sequence. Several experiments have been performed using different initial model definitions and the training strategies. The initial model definitions change according to the model topology (simple, triplet-word, or complex one), the total number of states, transition probabilities between the states, and the number of mixture of Gaussian used for each state. Applying the language modelling or context-dependent triphones states the training strategies.

As mentioned before, three different HMM topologies are used in the system:

- The simple system consists of 4 HMMs which are T, B, H, and C models.

- The triplet-word system consists of 60 HMMs which are the trio combinations of T, B, H, C, and X models.

- The complex system consists of 95 HMMs which are four combinations of T, B, H, C, and X words.

3.5.2.1 The Model with 4 HMMs

The simple model is built up of 4 HMMs which are T, B, H, and C models. We experimented performance with different extensions: adding the language model and applying triphone structures. The models have four or five states; their transition edges and probabilities are also different. For instance, there are some additional transition edges in the five states model. However, the five states model could not provide too much improvement on the recognition performance. Therefore, we do not provide the details of experiments used the five states model.

In the four states model, the initial transition matrix is given as follows:

$$
Transition\ matrix = \begin{bmatrix} 0 & 1.0 & 0 & 0 \\ 0 & 0.7 & 0.3 & 0 \\ 0 & 0 & 0.7 & 0.3 \\ 0 & 0 & 0 & 0 \end{bmatrix} \tag{3.6}
$$

The element 0.7 in the second row and second column indicates the associated transition probability a_{22}. In a similar way, there is no transition probability for the fourth state (the last row), due to be the end state of the model.

Basically, the acceptable recognition results are obtained with three models:

- Model 1: four states, two mixtures of Gaussian density (the first row of Table 3.2)

- Model 2: the language model is applied on four states, two mixtures of Gaussian density (the second row of Table 3.2)

- Model 3: the language model and the triphones are applied on four states, two mixtures of Gaussian density (the last row of Table 3.2)

For fairness, the results should be evaluated according to the MCC value. As said earlier, the Q_{total} sometimes may give unrealistic results due to low or high proportion of β-turn in protein sequence; hence, the MCC value should be used to determine the best performance.

The first model, four states with two mixtures of Gaussian density, has performed the best recognition with 0.045 MCC value, its $Q_{observed}$ performance is 25.95%. In other words, the model can find the correct location of β-turns with 26%. There is no effect of applying the language modelling and converting to the triphones to improve recognition performance. These results are not yet satisfactory for prediction of the location of β-turns.

Model Type	Q_{total}	$Q_{predicted}$	$Q_{observed}$	MCC
Model 1 *	65.71%	28.02%	25.95%	0.045
Model 2 †	71.17%	27.46%	11.13%	0.023
Model 3 ‡	67.86%	27.45%	19.38%	0.032

Table 3.2: The recognition performance of 4 states HMM with different extensions.

---

*Four states, two mixtures of Gaussian density
†In addition to first model, the language model is applied
‡In addition to second model, they are converted to the triphones

3.5.2.2 The Model with 60 HMMs

The triplet-word model is built up of 60 HMMs which are the trio combinations of T, B, H, C, and X models. This model has been developed to give the neighborhood relationship between simple words (secondary structures). We claim that the recognition performance of the system should be improved when introducing the trio combinations of simple words.

Several experiments have been done using the model with four and five states and adding the language model. The best recognition results are obtained by two models:

- Model 1: four states, two mixtures of Gaussian density (the first row of Table 3.3)

- Model 2: the language model is applied on five states, two mixtures of Gaussian density (the second row of Table 3.3)

The definition of the initial transition probabilities for the Model 1 (four states) is the same with the previous definition (see matrix 3.6). However, we used a different initialization for the Model 2 (five states), the transition probabilities of the Model 2 are given as follows:

$$
Transition\ matrix = \begin{bmatrix}
0 & 0.5 & 0.5 & 0 & 0 \\
0 & 0.6 & 0.2 & 0.2 & 0 \\
0 & 0 & 0.6 & 0.2 & 0.2 \\
0 & 0 & 0 & 0.6 & 0.4 \\
0 & 0 & 0 & 0 & 0
\end{bmatrix}
$$

The second model, consisting of five states with two mixtures of Gaussian density and using the language model, has performed the best recognition with 0.12 MCC value. Its $Q_{observed}$ performance is 33.57%; in other words the model could find the location of total β-turns correctly with 34% success. Applying the language model, giving bi-gram probabilities with dictionary file, improves the recognition performance. The MCC and $Q_{observed}$ value are 12% and 8% better than the previous results (see Table 3.2). Furthermore, the results are more satisfactory when compared to the 4 HMMs case.

Model Type	Q_{total}	$Q_{predicted}$	$Q_{observed}$	MCC
Model 1 [§]	66.04%	31.95%	34.81%	0.106
Model 2 [¶]	67.66%	33.64%	33.57%	0.124

Table 3.3: The recognition performance of 60 states HMM with different extensions.

3.5.2.3 The Model with 95 HMMs

The complex model is built up of 95 HMMs which are the four combinations of T, B, H, C, and X words. The topology of the complex model differs from the triplet-word model. Two fundamental information is wanted to introduce with this model: The first one is adding neighborhood relationship between the secondary structures by combining the four consecutive words; and the second one is forcing each model to capture β-turns rather than other secondary structures.

We made experiments using the model with three states and adding the language modelling. The best recognition results are obtained by two models:

- Model 1: three states, simple Gaussian density (the first row of Table 3.4)

- Model 2: the language model is applied on three states, simple Gaussian density (the second row of Table 3.4)

The definition of the initial transition probabilities for both model is given as follows:

$$Transition\ matrix = \begin{bmatrix} 0 & 1.0 & 0 \\ 0 & 0.6 & 0.4 \\ 0 & 0 & 0 \end{bmatrix}$$

The second model, consisting of three states with simple Gaussian density and the language model, has performed the best recognition with 0.11 MCC value. Its $Q_{observed}$ performance is 43.12% means that the model correctly finds the location of total β-turns with 43%. Applying the language modelling to give bi-gram probabilities improves the recognition performance. Even though the MCC value of complex

---

[§]Four states with two mixtures of Gaussian density
[¶]Five states with two mixtures of Gaussian density, the language model is applied

model is very close to the triplet-word model, the $Q_{observed}$ value of the complex model is 10% better than the triplet-word model (see Table 3.3).

Model Type	Q_{total}	$Q_{predicted}$	$Q_{observed}$	MCC
Model 1 $^{\parallel}$	67.60%	32.58%	30.80%	0.104
Model 2 **	63.36%	31.57%	43.12%	0.118

Table 3.4: The recognition performance of 95 states HMM with different extensions.

3.5.3 Discussion

We developed three different HMM topologies to compare their efficiency. The prediction performance of the simple model is very poor (Table 3.2). The simplicity of the model topology and the missing neighborhood information between secondary structures are the principle causes of that low prediction performance. Hence, the second model, the triplet-word, is developed; it combines the neighboring relations between the secondary structures and the robustness of a well-defined model. The triplet-models achieved more satisfactory predictions by adding bi-gram probabilities.

The complex model is developed to compare its accuracy to the triplet-word model. The complex model is constructed by combining four consecutive small models which are the simple words: T, H, B, and C. Although the complex model includes the small-size models, it is the biggest model in terms of the total number of HMMs. We obtained the highest percentage of correctly predicted β-turns (43%) with the complex model. Therefore, we can conclude that the initial claim for the complex model which forces the model to capture the β-turns has been verified.

In order to improve the performance of our HMMs, we may change the method of representing amino acid information. The HMMs can be trained by the multiple alignment profile scores instead of the amino acid similarity scores.

$^{\parallel}$Three states, simple Gaussian density
**Three states, simple Gaussian density, applying the language model

3.6 Summary and Conclusion

We have worked on the prediction of β-turns in protein sequences with different usage of HMMs. The critical role of β-turns on the folding pathway and limited research in literature have led us to work on the problem of identifying the location of β-turns in protein sequences. Furthermore, the absence of using HMMs in this problem enabled the application of HMMs as the prediction method.

There are two studies working on the prediction of β-turns with its amino acid sequence. The prediction technique, used data set, and feature of these studies are completely different with our work; however, they are the unique works for measuring the accuracy of our prediction system.

BTPRED is a neural network based approach [82]. They add to the input vector the secondary structure information of a given residue obtained from the PHDsec program [74]. The percentage of correctly predicted β-turns ($Q_{observed}$) and MCC (without applying filtering rules) value are 31% and 0.31, respectively. When we make a comparison of two methods, the MCC value of BTPRED is 19% better than our complex HMM's; however, the percentage of correctly predicted β-turns of the complex model is 12% better than those of BTPRED's. In BTPRED, the introducing predicted secondary structure information of each residue in the input vector significantly improved their performance. The absence of providing secondary structure information makes a negative effect on the performance of our HMMs.

BetaTPred2 also uses feedforward neural networks [43]. It includes two networks: first feedforward network with one hidden layer is trained using multiple sequence alignments in the PSI-BLAST form [1]. The second network is trained by the initial prediction of the first network and PSIPRED secondary structure information [39]. They provide a significant improvement by giving evolutionary information with PSI-BLAST multiple alignments. The percentage of correctly predicted β-turns and MCC value are 72% and 0.43, respectively. The performance of our HMMs could not achieve the high performance of the BetaTPred2. It is known that using information from sequence alignments improves the secondary structure predictions. PSI-BLAST, an improved searching tool for multiple sequence alignment, searches the homologous proteins against a larger database. Hence, the essen-

tial reason for the high performance of BetaTPred2 is its ability to give evolutionary information effectively.

In this study, we observed the insufficiency of amino acid similarity score against the multiple alignment profile scores. Even though we tried to introduce the neighborhood information between secondary structures by combining simple words (T,H,B,C), we could not introduce the evolutionary information properly. Furthermore, the prediction errors of the α-helix, β-sheet, and coil regions have contributed the prediction errors of β-turns; so, if we could construct a model consisting of the β-turn and non-turn words, we would eliminate the error resulting from the α-helices, β-sheets, and coils.

Actually, HMM has performed the prediction of β-turns merely using the amino acid similarity scores quite well. If we had used the PSI-BLAST multiple alignment scores instead of the amino acid similarity scores, the prediction performance of the HMM would have been much better. As an initial work, we obtained promising results for the β-turn prediction problem using HMMs.

3.7   Usage of Hidden Markov Model Toolkit

The Hidden Markov Model Toolkit (HTK) is applied to predict the location of β-turns in a given protein sequence [32]. The HTK is a portable toolkit for building and manipulating HMMs. HMMs can be used to model any time series and the core of HTK is similarly general-purpose. HTK is primarily used for speech recognition research although it has been used for numerous other applications including research into speech synthesis, character recognition and DNA sequencing.

There are two major processing stages involved. Firstly, the HTK training tools are used to estimate the parameters of a set of HMMs using training utterances and their associated transcriptions. Secondly, unknown utterances are transcribed using the HTK recognition tools.

HTK is built into the library modules. These modules ensure that every tool interfaces to the outside world in exactly the same way. They also provide a central resource of commonly used functions. Figure 3.7 illustrates the software structure

of a typical HTK tool and shows its input/output interfaces.

We have prepared our data (the protein sequences) without using HTK libraries. Therefore, we just mention about the training and recognition libraries of HTK. Figures and review is taken from the HTK user manual [32].
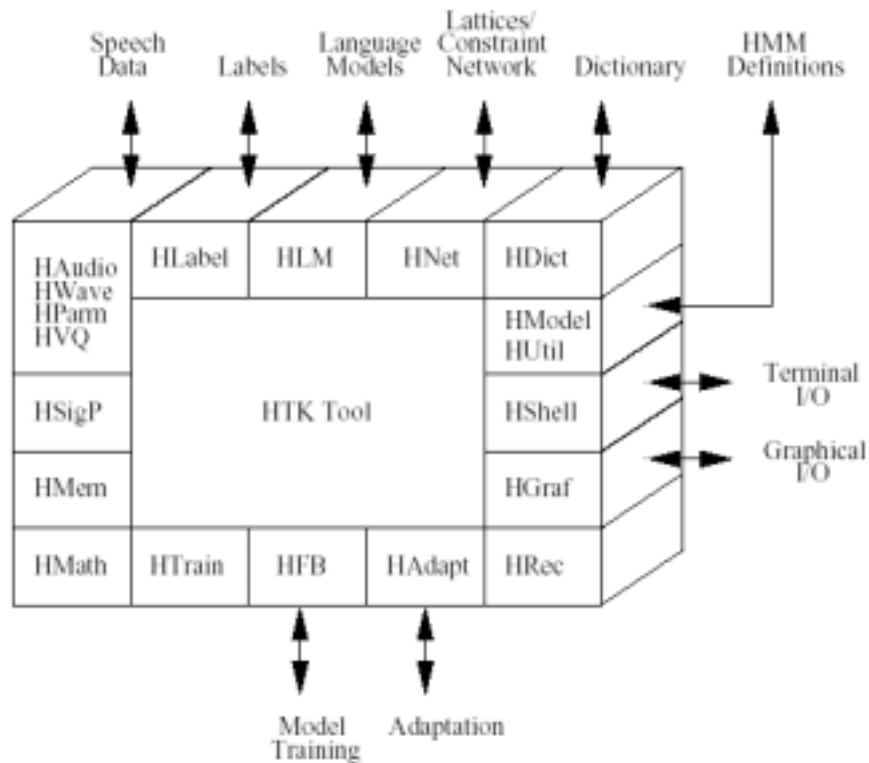
Figure 3.7: HTK software architecture.

3.7.1 Training Libraries

After preparing data (protein data files and their transcriptions), the second step of system building is to define the topology required for each HMM by writing a prototype definition. HTK allows HMMs to be built with any desired topology. HMM definitions are be stored as simple text files. The purpose of the prototype definition is only to specify the overall characteristics and topology of the HMM. The actual parameters will be computed later by the training tools. Sensible values for the transition probabilities must be given but the training process is very insensitive to these. An acceptable and simple strategy for choosing these probabilities is to make all of the transitions out of any state equally likely.

Firstly, an initial set of models must be created. If there is some data available for which the location of the sub-word (secondary structure elements) boundaries have been marked, then this can be used as bootstrap data. In this case, the tools HInit and HRest provide isolated word style training using the fully labelled bootstrap data. Each of the required HMMs is generated individually. HInit reads in all of the bootstrap training data and cuts out all of the examples of the required phone. It then iteratively computes an initial set of parameter values using a segmental k-means procedure. On the first cycle, the training data is uniformly segmented, each model state is matched with the corresponding data segments and then means and variances are estimated. If mixture Gaussian models are being trained, then a modified form of k-means clustering is used. On the second and successive cycles, the uniform segmentation is replaced by Viterbi alignment. The initial parameter values computed by HInit are then further re-estimated by HRest. Again, the fully labelled bootstrap data is used but this time the segmental k-means procedure is replaced by the Baum-Welch re-estimation procedure.
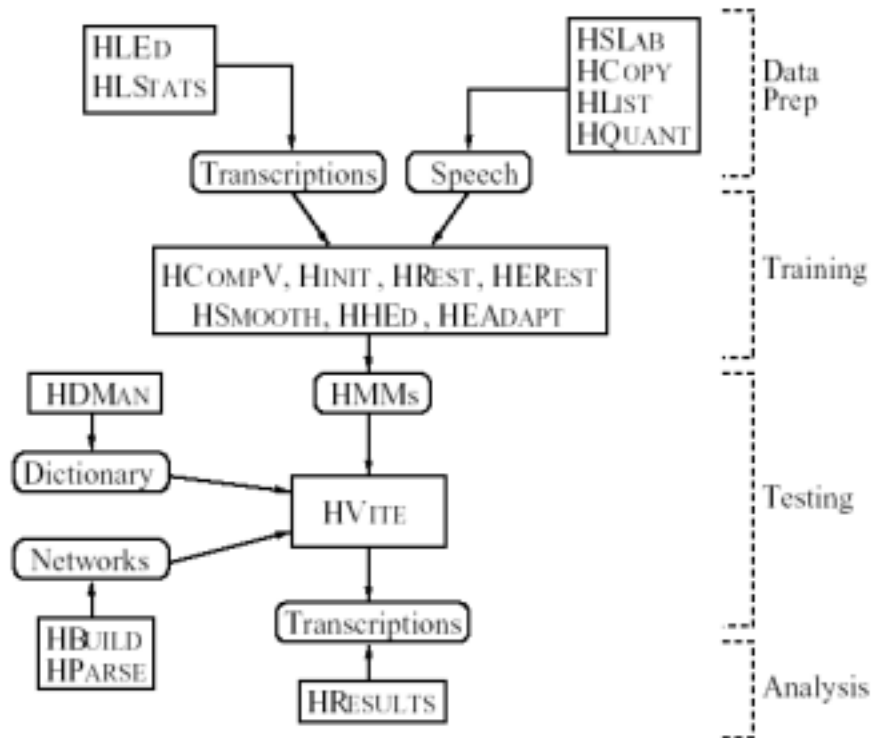
Figure 3.8: HTK processing stages.

46

Once an initial set of models has been created, the tool HERest is used to perform embedded training using the entire training set. HERest performs a single Baum-Welch re-estimation of the whole set of HMM phone models simultaneously. For each training utterance, the corresponding models are concatenated and then the forward-backward algorithm is used to accumulate the statistics of state occupation, means, variances, etc., for each HMM in the sequence. When all of the training data has been processed, the accumulated statistics are used to compute re-estimates of the HMM parameters. The philosophy of system construction in HTK is that HMMs should be refined incrementally. Thus, a typical progression is to start with a simple set of single Gaussian context-independent models and then iteratively refine them by expanding them to include context-dependency and use multiple mixture component Gaussian distributions. The tool HHEd is an HMM definition editor which will clone models into context-dependent sets, apply a variety of parameter tyings and increment the number of mixture components in specified distributions. The usual process is to modify a set of HMMs in stages using HHEd and then re-estimate the parameters of the modified set using HERest after each stage. The more complex the model set, the more data is needed to make robust estimates of its parameters, and since data is usually limited, a balance must be struck between complexity and the available data.

3.7.2 Recognition Libraries

The HTK tool can perform the Viterbi-based recognition. It takes the word network and then attaches the appropriate HMM definition to each word instance. Then the recognition is performed on the list of test files. HTK provides a single recognition tool called HVite which uses the token passing algorithm to perform Viterbi-based recognition. HVite takes as input a network describing the allowable word sequences, a dictionary defining how each word is pronounced and a set of HMMs. According to speech terminology, a word is pronounced as the sequence of phones p1 p2 p3 etc. Hence, the dictionary file keeps all possible words and their pronunciations. For β-turn prediction problem, no need to give pronunciation of words (T, H, B, C) in a special way; because, we don't want to find the pronunciation of a given

word or vice versa. Actually, the aim is to identify the words (T, H, B, or C) of a given protein sequence; so, we leave pronunciations the same with words. HVite operates by converting the word network to a phone network and then attaching the appropriate HMM definition to each phone instance. Recognition can then be performed on the list of stored test files. HVite can support cross-word triphones and it can run with multiple tokens to generate lattices containing multiple hypotheses. The word networks needed to drive HVite are usually either simple word loops in which any word can follow any other word or they are directed graphs representing a finite-state task grammar. In the former case, bi-gram probabilities are normally attached to the word transitions.

HBuild allows sub-networks to be created and used within higher level networks. HBuild can be used to generate word loops and it can also read in a backed-off bi-gram language model and modify the word loop transitions to incorporate the bi-gram probabilities. Note that the label statistics tool HLStats can be used to generate a backed-off bi-gram language model. As an alternative to specifying a word network directly, a higher level grammar notation can be used. This notation is based on the Extended Backus Naur Form (EBNF) used in compiler specification and it is compatible with the grammar specification language. The tool HParse is supplied to convert this notation into the equivalent word network.

3.7.3   Language Modelling

A described in the previous section, HTK tool needs a network describing the allowable word sequences, during the recognition phase. The word networks needed to drive either simple word loops in which any word can follow any other word or they are directed graphs representing a finite-state task grammar. The bi-gram probabilities are attached to the word transitions and they provide a prior information about the consecutive word relations. In order to calculate the bi-gram probabilities we should apply the language modelling to the training data.

The HTK language modelling tools are designed for constructing and testing statistical n-gram language models. An n-gram is a sequence of n symbols and an n-gram language model (LM) is used to predict each symbol in the sequence given

its n-1 predecessors. It is built on the assumption that the probability of a specific n-gram occurring in some unknown test text can be estimated from the frequency of its occurrence in some given training text.

The n-gram construction is a three stage process. Firstly, the training text is scanned and its n-grams are counted and stored in a database of gram files. In the second stage some words may be mapped to an out of vocabulary class or other class mapping may be applied, and then in the final stage the counts in the resulting gram files are used to compute n-gram probabilities which are stored in the language model file. Lastly, the goodness of a language model can be estimated by using it to compute a measure called **perplexity** on a previously unseen test set. In general, the better a language model then the lower its test-set perplexity. Although the basic principle of an n-gram LM is very simple, in practice there are usually many more potential n-grams than can ever be collected in a training text in sufficient numbers to yield robust frequency estimates. If the LM is word-based, it can only predict words within its vocabulary; furthermore, new words cannot be added without rebuilding the LM.

The prior probability $P(w_i)$ is used in the Bayes formula as follows:

$$P(w_i|O) = \frac{P(O|w_i) \, P(w_i)}{P(O)} \tag{3.7}$$

The most probable observed word depends only on the likelihood $P(O|w_i)$. Language models estimate the probability of a word sequence, $\hat{P}(w_1, w_2, \cdots, w_m)$ which can be decomposed as a product of conditional probabilities:

$$\hat{P}(w_1, w_2, \cdots, w_m) = \prod_{i=1}^{m} \hat{P}(w_i|w_1, \cdots, w_{i-1}) \tag{3.8}$$

Equation 3.8 presents an opportunity for approximating $\hat{P}(W)$ by limiting the context:

$$\hat{P}(w_1, w_2, \cdots, w_m) \simeq \prod_{i=1}^{m} \hat{P}(w_i|w_{i-n+1}, \cdots, w_{i-1}) \quad for \; n \geq 1 \tag{3.9}$$

If language has a property that the probability of any state can be estimated from a large enough history independent of the starting conditions, then for suffi-

ciently high n equation 3.8 is true. Models using contiguous but limited context in this way are usually referred to as n-gram language models, and the conditional context component of the probability $(w_{i-n+1}, \cdots, w_{i-1})$ is referred to as the history.

Estimates of probabilities in n-gram models are based on maximum likelihood estimates by counting events in context on some given training text:

$$\hat{P}(w_i|w_{i-n+1}, \cdots, w_{i-1}) = \frac{C(w_i, \cdots, w_{i-1})}{C(w_{i-n+1}, \cdots, w_{i-1})} \qquad (3.10)$$

where C(.) is the count of a given word sequence in the training text. There are some refinements for this maximum likelihood estimate, but we do not go into more details.

There is a support for statistical language models in HTK. Although the interface to LM can support general n-grams, the facilities for constructing and using n-grams are limited to bi-grams. A bi-gram language model is built using HLStats invoked by a text file which includes all of the label files and a word list of all words used in the label files. In our case we marked all protein files using secondary structure element names and formed a word list file which includes those secondary structure element names. After calculation of bi-gram of our words, the HBuild makes a word-level network using the output bi-gram file of HLStats program.

3.7.4 Context-Dependent Triphones

In this section, we used the terms *phone* or *monophone* instead of our words T (turn), H (helix), B (sheet), and C (coil). The one method of model refinement is usually to convert a set of initialised and trained context independent monophone HMMs to a set of context dependent models. Context-dependent triphones can be made by simply cloning monophones and then re-estimating using triphone transcriptions.

HTK uses the convention that an HMM name of the form 'l-p+r' denotes the context-dependent version of the phone 'p' which is to be used when the left neighbour is the phone 'l' and the right neighbour is the phone 'r'. To make a set of context dependent phone models, it is only necessary to construct an HMM list, called triphone list, containing the required context-dependent models and then

execute HHEd program that makes a copy of the monophone 'p' for each model 'l-p+r' in triphone list. The set of context-dependent models output by the above must be re-estimated using HERest. To do this, the training data transcriptions must be converted to use context-dependent labels and the original monophone hmm list must be replaced by triphone list. In fact, it is best to do this conversion before cloning the monophones because the HLEd program can be used to generate the required list of context dependent HMMs automatically.

Before building a set of context-dependent models, it is necessary to decide whether or not cross-word triphones are to be used. Tying could affect performance if performed indiscriminately. Hence, it is important to only tie parameters which have little effect on discrimination. If the transition parameters do not vary significantly with context but nevertheless need to be estimated accurately. Some triphones will occur only once or twice and so very poor estimates would be obtained if tying was not done. These problems of data insufficiency will also affect the output distributions.

Chapter 4

The Classification of The β-Turns by Artificial Neural Networks

4.1 Introduction

The β-turns are not unified structures; they include different types. Hence, identifying the location of the β-turns in protein sequence is insufficient; type of β-turns would also be useful. Even though there are few studies on identification of the β-turn regions, the work on identifying the type of the β-turns is even more limited. We have attempted to find the location of β-turns using HMMs in Chapter 3. As a second step, we wanted to extend this study on type classification of β-turns by using Artificial Neural Networks.

The critical roles of β-turns on the protein fold should not be underestimated since the β-turns comprise on the average 25% of the residues in the globular proteins [40] and change the direction of the amino acid chain. In addition, β-turns reside on the surface of the protein and interact with other proteins or molecules; hence the identification of the location and type of the β-turns may give clues about the interaction of a protein with other proteins.

4.2 Types of β-Turns

Among the tight turns, β-turns are the most common ones, formed by four consecutive residues (R_i, R_{i+1}, R_{i+2}, R_{i+3}). The most commonly used definition of β-turns is the following: "It must comprises four consecutive residues where the distance between $C\alpha_i$ and $C\alpha_{i+3}$ is less than $7\mathring{A}$ and tetrapeptide chain is not in a helical conformation" [70, 73].

β-turns have been classified into nine different types (I, I', II, II', VIa1, VIa2, VIb, IV, VIII) based on the dihedral angles of the inner residues at positions i+1 and i+2 [34, 70, 89]. The illustration of each type is given in Figure 4.1 and the mean dihedral angles of each β-turn type is also given in Table 4.1. The angle values for type VI turns are taken from Richardson [70], and the rest were determined by Lewis et.al. [53].

Angles Type	$\phi(i+1)$	$\psi(i+1)$	$\phi(i+2)$	$\psi(i+2)$
I	-60	-30	-90	0
I'	60	30	90	0
II	-60	120	80	0
II'	60	-120	-80	0
IV	-61	10	-53	17
VIa1	-60	120	-90	0
VIa2	-120	120	-60	0
VIb	-135	135	-75	160
VIII	-60	-30	-120	120

Table 4.1: The mean dihedral angles for β-turn types.

4.3 Previous Work

The criteria to define the type of a β-turn is the backbone dihedral angles; but if the 3D structure information of a protein is unknown, the type of β-turns in this protein cannot be determined directly. Hence, the development of classification methods to identify the type of β-turns of a given amino acid sequence is necessary. Some statistical approaches identify the β-turn residues of a given amino acid sequence, however, they do not classify the β-turn types [18, 34, 94].
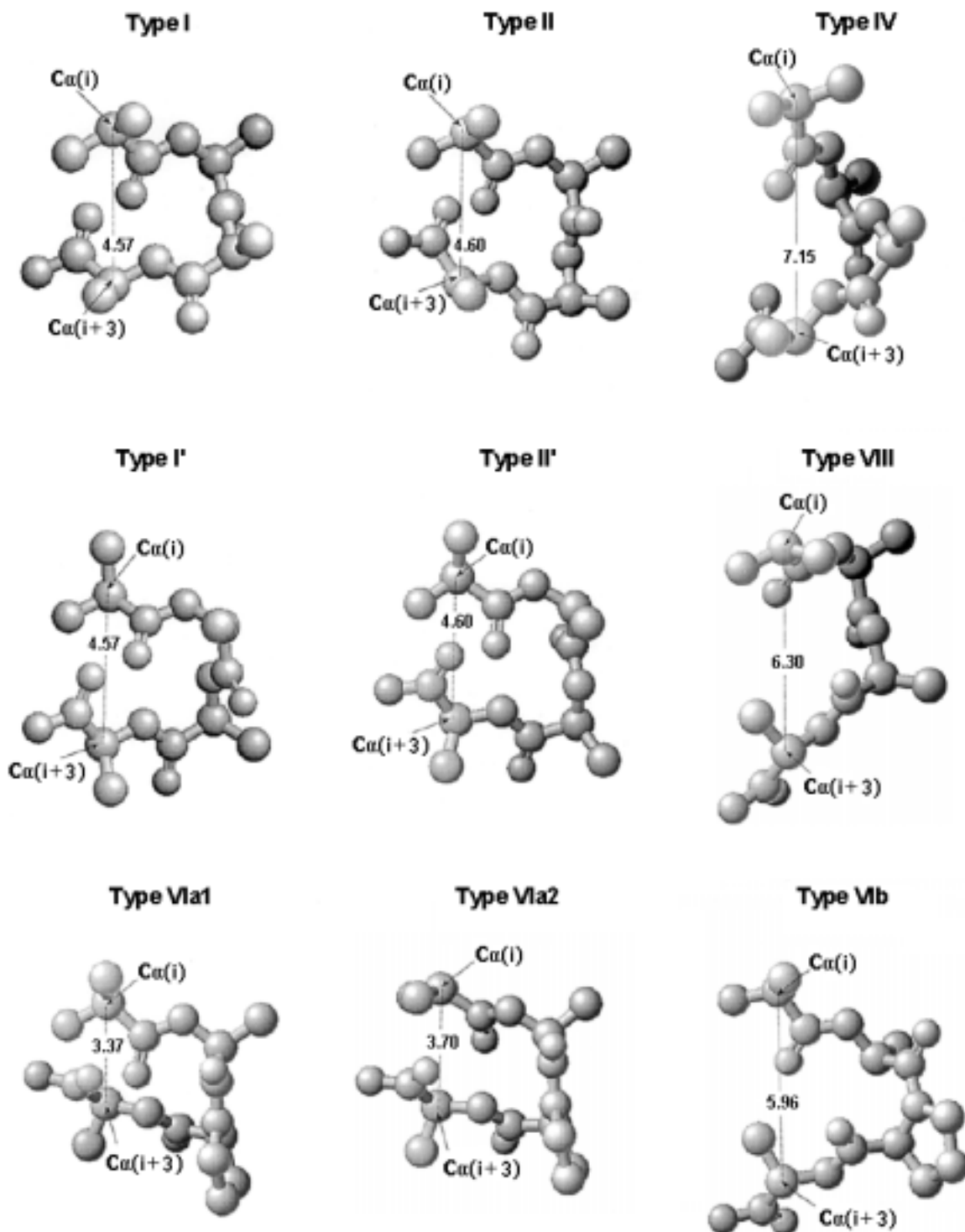
Figure 4.1: The illustration of the nine different types of β-turns. The first and fourth main carbon atoms are marked. The distance between these two atoms is also given. (The image of each β-turn type is taken from Chou [16].)

Two studies working on the classification of the β-turn types are noteworthy. The first one is **BTPRED** which is a neural network based method using a feedforward neural network with one hidden layer [82]. The input vector is formed using binary encoding. In other words, each amino acid is represented by a single one and nineteen zeros, giving an 80 dimensional input vector. In addition, they use the secondary structure information (α-helix, β-sheet or coil) obtained from the PHDsec program. So, the total dimension of their input vector increases to 83. The β-turn type classification performance is different for each class because of the unbalanced data in each class. Their average test performance for the four β-turn types is near 36%.

The second work classifying the type of β-turns uses SVM as the classification tool [11]. As in the previous work, the input vector is formed using binary encoding; each β-turn is represented by an 80 dimensional vector. The β-turn type classification performance (training performance) is 98% on the average. However, this performance is obtained from the *training data*, no test performance was given.

4.4 Our Method

A **Multilayer Perceptron** (MLP) is used to classify the type of β-turns. MLPs are one of the commonly used types of Artificial Neural Networks (ANN) for the supervised classification tasks. The detail information about ANNs and the training algorithm is explained in Appendix C.

In this study, the MLP consists of an input layer, one hidden layer, and an output layer. The input vector, representing a β-turn sequence, is feed to the input layer of the MLP and the network is trained to output the type (class) of this β-turn. The input vector has 12, 17, or 18 dimensions. The content of each one will be explained in Section 4.4.2. The number of neurons for the hidden layer varies between 10 and 20. The number of the output nodes is the total number of β-turn classes using the one-of-c encoding for the classification, as shown in Figure 4.2. The target value of output nodes is assigned to 0.9 for the desired class, and 0.1 for other classes. A threshold is set to decide when the winning node's activation

is high enough to be considered valid; if the activation of all output nodes are close to zero, there would no a valid class assignment. When the output of the winning neuron (highest activation) is bigger than 0.6, the input is considered to belong to that class.

The activation function of the hidden layer and output layer is the sigmoidal function. Sigmoidal functions provide a smooth, continuous version of threshold function, which are differentiable. The learning rate (η) which is a constant regulating the amount of change to the network parameters, ranges from 0.05 - 0.5. The momentum (α) which is an extra parameter smoothing out the erratic behaviour of the weight updates, is between 0.1 - 0.9.
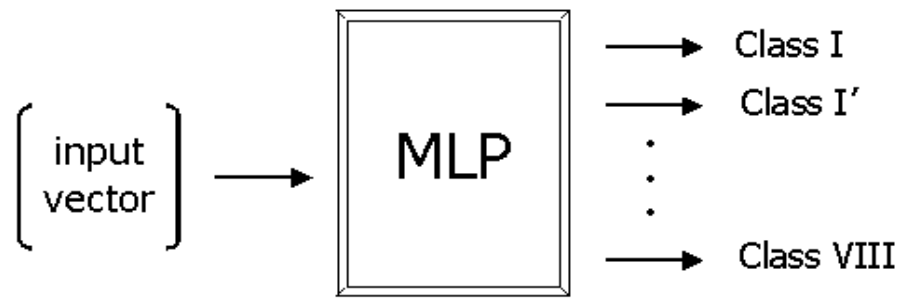
Figure 4.2: The illustration of the process flow in our MLP.

We have applied the backpropagation algorithm to train the MLP. Training an MLP is an iterative process that involves repeatedly presenting the training set to the network. The error function of the network is the mean squared error (MSE). After each presentation the MLP parameters (weights) are adjusted so that the networks MSE for all patterns in the set is progressively reduced. This type of training is called **supervised learning** and the algorithm for adjusting the MLP weights is the training method. One method for training MLPs is backpropagation which derives from the oldest and simplest of classical optimization techniques, steepest descent (for details see Appendix C).

4.4.1 Data Set

The data set, which is the same as the one used in Chapter 3, is composed of 1190 training and 163 test protein chains. The construction details were explained in Chapter 3 (Section 3.4.2).

We used the PROMOTIF program [35] to classify the extracted β-turns into the nine known types (I, II, I', II', VIa1, VIa2, VIb, IV, VIII). Types I, II, I', II', and VIII meet the structural requirement of the β-turn definition. The β-turn types VIa1, VIa2, and VIb can be seen when the third residue is proline and $\psi(i+1)$ is $0°$. In addition, the β-turn type IV does not satisfy the β-turn definition (the distance between $C_\alpha(i)$, and $C_\alpha(i+3)$ is higher than 7Å); so, type IV is called a miscellaneous category.

In our data set, the total number of samples for VIa1, VIa2, and VIb types were very small (less than 1% of data set); hence, they are collected into one class, called the VI type. The training set includes 16644 β-turns, the test set includes 1879 β-turns. The frequency of each β-turn type is given in Table 4.2.

β-Turn type	Training		Test	
	Number	%	Number	%
I	5488	32.9	619	32.9
I'	609	3.6	73	3.8
II	1794	10.7	201	10.6
II'	353	2.1	57	3
IV	6705	40.2	756	40.2
VI	276	1.6	30	1.5
VIII	1419	8.5	143	7.6
Total	16644	100	1879	100

Table 4.2: The frequency of each β-turn type for the training and test data sets.

4.4.2 Feature Sets

The feature vector is composed by the β-turn sequence which has four residues. There are three different features used in constructing the input vector: amino acid similarity score, size ratio, and hydrophobicity.

- **Similarity score**: We used a 3D similarity vector that is formed by reducing the dimensions of the PAM250 similarity matrix [36]. The details of the construction are explained in Chapter 3 (Section 3.4.3).

- **Size ratio**: The size information of amino acids is critical for β-turns because of the bond between first and fourth residues. The size of the first and fourth residue should be close to make a strong bond. In other words, their relative size should not be too big or too small, but proportional. For instance, if both of them were too big amino acids to make a bond, they would crash and not make a proper bond. Hence, we use the size ratio to compare the size of these critical residues. Actually, the size measure is the **surface area** of each amino acid given in Table 4.3 [4].

Amino Acid	Surface Area	Hydrophobicity
C	134.28	4.77
G	80.10	0
P	136.13	-2.01
S	116.50	-1.51
A	107.95	0.50
T	139.27	-0.5
D	140.39	-2.51
E	172.25	-2.51
N	143.94	-2.26
Q	178.50	-2.51
H	182.88	1.51
K	200.81	-5.03
R	238.76	-2.01
V	151.44	3.52
M	194.15	3.27
I	175.12	4.02
L	178.63	3.27
F	199.48	4.02
Y	212.76	1.01
W	249.36	3.27

Table 4.3: The surface area and hydrophobicity features of each amino acid.

- **Hydrophobicity**: β-turns usually contain polar and charged residues. The most frequent pattern of residues observed is that form: hydrophobic, hydrophilic, hydrophilic, and hydrophobic. Therefore, we also apply the hy-

drophobicity feature to consider that information. The hydrophobicity value of each amino acid is also given in Table 4.3.

Three different input vectors with different dimensions are constructed. Before using input vectors, they are normalized to have zero mean and unit variance. Each input vector includes the following features:

- 12 dimension: includes only the amino acid similarity scores. A β-turn consists of four residues and the 3D similarity score is used for each one.

- 17 dimension: Addition to amino acid similarity scores (12), the size ratio of the first and fourth residues (1), and the hydrophobicity value of each residue (4) are also used.

- 18 dimension: The amino acid similarity scores (12), the size ratio of the first and fourth residues (1), the size ratio of the second and third residues (1), and the hydrophobicity value of each residue (4) are used.

4.5   Results and Discussion

We have performed the training and test for three different cases by using the following input vectors:

1. 12 dimensional

2. 17 dimensional

3. 18 dimensional

Although the classification performances of the 17D and 18D vectors are very similar, the 17D input vector performed the best one. The sigmoid and tangent activation functions in the MLP layers provide identical performance. The detailed results will be given in the following sections.

4.5.1 Training and Test Performance

4.5.1.1 Using the 12D input vector

We have tried to measure the classification performance of the MLP using the amino acid similarity scores for representing β-turns. We know that some key amino acids have a very strong effect on the folding of β-turns, so we can partially predict the class of β-turns by using amino acid similarity scores.

The best average test performance of the neural network is 51% using the 12D input vector, as shown in Table 4.4. The classification performance of the network is not the same for each type of β-turns. For instance, both training and test performance is 0% for type II'. This result is a known fact about type II' turns which cannot be classified easily (also in other works). Another poor result belongs to type VIII turns whose test performance is also 0%. The network could not achieve the classification of type VIII turns.

The correct classification percentage of each class (for the best run) is given in Table 4.4. The confusion matrix of each class can be seen in Table 4.5. Several results of the network runs with different parameters are given in Table 4.6.

β-turn type	Training %	Test %
I	55.9	37.9
I'	28	36.9
II	62.4	64.7
II'	0	0
IV	58.9	70.4
VI	100	100
VIII	0.7	0
Avg:	51.5	50.7

Table 4.4: The correct classification rate of each type of β-turns using the 12D input.

4.5.1.2 Using the 17D input vector

In addition to the amino acid similarity scores, we also experimented with the effects of the size ratio and hydrophobicity features on the classification performance of the MLP. In order to construct stronger β-turn structures, the size of the first and fourth

	I	I'	II	II'	IV	VI	VIII
I	-	-	25	-	354	6	-
I'	1	-	16	-	29	-	-
II	17	10	-	-	44	-	-
II'	-	1	1	-	55	-	-
IV	128	6	72	-	-	18	-
VI	-	-	-	-	-	-	-
VIII	28	-	-	-	116	-	-

Table 4.5: The count of the confused data for the test results in Table 4.4.

# Epoch	η	α	Train MSE	Train %	Test MSE	Test %	# Hid. Node
1000	0.1	0.5	0.0558	50.35	0.0570	48.25	8
1000	0.1	0.9	0.0558	50.46	0.0566	48.09	8
1000	0.05	0.5	0.0554	50.94	0.0561	49.79	10
1000	0.1	0.1	0.0552	51.71	0.0562	50.11	10
1000	0.07	0.9	0.0552	51.50	0.0559	50.70	12
1000	0.1	0.9	0.0552	51.71	0.0562	50.27	12

Table 4.6: The network results using the 12D input vector. The term "Train %"refers to the ratio of the correctly classified β-turns to the total number of β-turns in the training set. The term "Test %"refers to the ratio of the correctly classified β-turns to the total number of β-turns in the test set.

residue must be close to each other. We take the surface area ratios of that two residues to compare their size. Furthermore, the hydrophobic amino acids present the start and end of the β-turns; the hydrophilic amino acids present in the middle of the β-turns. Therefore, we also add the hydrophobicity feature into the input vector.

The best average test performance of the network is 53%, using the 17D input vector, as shown in Table 4.7. There is an increase on the average performances for both training and testing phases. We explain this increase by adding the size ratio and hydrophobicity features into the input vector.

As before, the classification performance of the network is not the same for each type of β-turns. Actually, the network has very a small ability (0.2 - 0.3%) to classify type II' and VIII turns during the training. However, the test performance of the network for two type is 0%, so these poor performances continue for that case as similar with the 12D input vector usage.

The correct classification percentage of each class (for the best run) is given

in Table 4.7. The confusion matrix of each class can be seen in Table 4.8. Several results of the network runs with different parameters are given in Table 4.9.

β-turn type	Training %	Test %
I	60.8	59.3
I'	30.3	34.3
II	63.8	67.2
II'	0.3	0
IV	56.7	58
VI	96.4	100
VIII	0.2	0
Avg:	52.5	52.9

Table 4.7: The correct classification rate of each type of β-turns using the 17D input.

	I	I'	II	II'	IV	VI	VIII
I	-	1	26	-	218	7	-
I'	7	-	20	-	21	-	-
II	15	8	-	-	43	-	-
II'	6	1	1	-	47	2	-
IV	210	7	82	-	-	19	-
VI	-	-	-	-	-	-	-
VIII	31	-	1	-	112	-	-

Table 4.8: The count of the confused data for the test results in Table 4.7.

# Epoch	η	α	Train MSE	Train %	Test MSE	Test %	# Hid. Node
1000	0.05	0.5	0.0543	52.54	0.0545	52.93	12
1000	0.1	0.9	0.0543	52.53	0.0546	52.14	12
1000	0.1	0.1	0.0544	53.05	0.0553	51.71	14
1000	0.1	0.9	0.0543	52.75	0.0557	50.86	14
1000	0.1	0.1	0.0541	53.26	0.0554	50.59	15
1000	0.1	0.9	0.0540	53.00	0.0550	52.24	15

Table 4.9: The network results using the 17D input vector.

4.5.1.3 Using the 18D input vector

We have done a new addition, another size ratio, to the input vector. In addition to the amino acid similarity scores, the size ratio of first and fourth residue, and hydrophobicity features, we wanted to experiment the effect of the size ratio of the second and third residues. Hence, we take the surface area ratios of the second and third residues to compare their size.

The best average test performance of the network is 52%, using the 18D input vector, as shown in Table 4.10. The performance of the network is very close to the performance of using the 17D input vector that is not particularly useful this size ratio of the second and third residue.

The classification performance of the network again is not the same for each type of β-turns. The network has a small ability (2 - 4.6%) to classify type II' and VIII turns during the training. The test performance of the network is 0% and 3.5% for type II' and VIII, respectively. We measured a little improvement for type VIII turns using the 18D input vector.

The correct classification percentage of each class (for the best run) is given in Table 4.10. The confusion matrix of each class can be seen in Table 4.11. Several results of the network runs with different parameters are given in Table 4.12.

β-turn type	Training %	Test %
I	60.4	63.5
I'	29.4	39.8
II	40.4	66.2
II'	2	0
IV	59.1	52.6
VI	97.2	86.7
VIII	4.6	3.5
Avg:	53.5	52.2

Table 4.10: The correct classification rate of each type of β-turns using the 18D input.

	I	I'	II	II'	IV	VI	VIII
I	-	1	24	-	192	6	3
I'	4	-	20	-	20	-	-
II	22	10	-	-	36	-	-
II'	9	1	1	-	46	-	-
IV	247	12	78	-	-	14	8
VI	2	-	-	-	2	-	-
VIII	41	-	-	-	98	-	-

Table 4.11: The count of the confused data for the test results in Table 4.10.

# Epoch	η	α	Train MSE	Train %	Test MSE	Test %	# Hid. Node
1000	0.05	0.1	0.0536	53.52	0.0549	52.29	16
1000	0.07	0.9	0.0539	53.71	0.0551	52.19	16
1000	0.1	0.5	0.0541	53.67	0.0554	51.87	16
1000	0.07	0.9	0.0535	54.14	0.0558	51.44	18
1000	0.1	0.1	0.0537	54.14	0.0562	51.76	18
1000	0.1	0.9	0.0540	53.71	0.0564	50.11	18

Table 4.12: The network results using the 18D input vector.

4.5.2 Discussion

We have made several experiments with different network topologies (the number of hidden nodes, learning rate etc.) and input vectors (12D, 17D, and 18D) to obtain a better classification performance for the type of β-turns.

The network performance has changed for each β-turn type. The performance is much better for types I, II, and VI, especially. The content of the input vector is not sufficient in order to classify the other β-turn type. Most of the time, the network could not classify any data in type VIII. The reason for the low performance might be the small number of data for type VIII turns. In addition, type VIII turns are characterized by a high degree of conformational variability.

4.6 Summary and Conclusion

There are two similar studies whose classification performance can be compared to ours. The correct classification percentage of each β-turn type for all studies is given in Table 4.13.

The classification performance of BTPRED is about the same as ours [82]. Actually, the performance of our network is better than their results except for type VIII. The main difference between the two studies is the input vector composition; because they used the binary representation of each amino acid; so, they had an 80 dimensional input vector. In addition, their data set including 3359 β-turns is smaller than ours.

Another similar research belongs to Cai et.al. [11]. They use SVMs as the classification method and their input vector is the same as Shepherd et.al. However, there is no test performance in their results. They only report the training (the self-consistency in their terms) results. In order to make a realistic comparison we need to know their test performance. In addition, our data set is completely different from their data set. We could not achieve their training performance using our MLP. The reasons for their better training performance might be the usage of data set where the protein sequence identity is higher than 25% or applying SVMs as the classification tool.

The classification algorithm and the composition of input vector are the most important factors to classify the type of β-turns. We could not construct more powerful input vector which can capture the difference between each β-turn type exactly by using merely protein sequence information. Another possible source for the low performance may be the ANN: although ANNs are universal function approximators and have proven to be very successful in many complex problems, a network may not learn if the network does not have enough capacity or it may not generalize if there is not enough training data or the training data is not representative of the test data. Hence, another classification algorithm can be applied on the same problem. Support Vector Machines are applicable to regression and classification tasks where they have consistently shown higher performance than traditional learning tools. Hence, SVMs might be a candidate to classify the type of β-turns.

βturn type	Cai's result[1]	Shepherd's result[2]	Our result[3]
I	99.9%	48.0%	59.3%
I'	96.8%	-	34.3%
II	98%	60.3%	67.2%
II'	97.7%	-	0
IV	100%	9.4%	58%
VI	100%	-	100%
VIII	97.1%	21.5%	0
Average:	98%	36%	53%

Table 4.13: The performance comparison of the previous β-turn type classification works to our method. [1]The *training performance* of Cai et.al. [11]. [2]Test performance of Shepherd et.al. [82]. The '-' represents the unreported result. [3]Test performance of our network which is trained by the 17D input vector.

Appendix A

Support Vector Machines

SVM is a relatively new pattern classification technique, based on statistical learning theory [8, 20, 80, 88]. The idea behind the SVM theory exists since the 1960s but crucial development of SVM has been realized in the 1990s [20]. SVMs are applicable to regression and classification tasks where they have consistently shown higher performance than traditional learning tools (especially for classification problems).

The basic idea of SVMs for pattern classification can be stated as follows. SVM maps the input space into a higher dimensional feature space. Mapping can be done either linearly or non-linearly, according to the kernel function used for the mapping (Figure A.1 depicts a non-linear mapping done with a SVM). In this new feature space, the SVM constructs separating hyper planes that are optimal in the sense that the classes are separated with the largest margin and minimum classification error. The optimal hyper plane can be written as a combination of a few feature points those are called the **support vectors** of the optimal hyper plane. The following description of the SVM and Figures A.2, A.3) are taken from Burges [8].
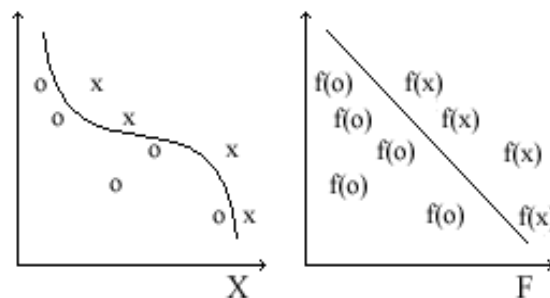

Figure A.1: Data points are mapped into a feature space where they are linearly separable.

A.1   The linearly separable case

SVMs are mainly designed for 2-class classification problems. Given the input points x_i belonging to two classes, we can associate one class with the output 1 and the other with the output -1, such that:

$$\{\mathbf{x}_i, y_i\}, \; i = 1, ..., l, \; y_i = \{-1, +1\}, \; \mathbf{x}_i \in \mathbf{R}^d \tag{A.1.1}$$

We can construct hyper planes separating the 1-class (filled dots) from the -1-class (open dots), as indicated in Figure A.2. The points $\mathbf{x}$ which line on the hyper plane satisfy $\mathbf{w} \cdot \mathbf{x} + b = 0$ where $\mathbf{w}$ is normal to the hyper plane and $|\mathbf{w}|$ is the Euclidean norm of $\mathbf{w}$.
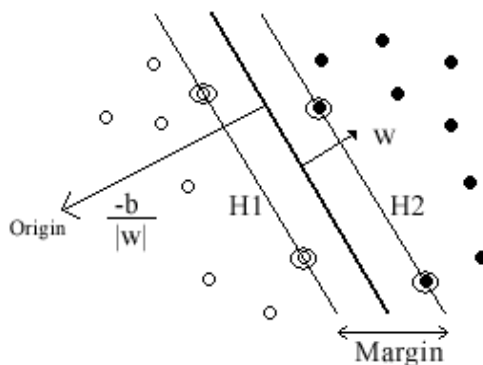

Figure A.2: Linear separating hyperplanes for the separable case. The support vectors are H1 and H2.

The shortest distance from the separating hyper plane, H1 or H2, to the closest 1/-1 example is called the **margin**. The support vector algorithm seeks for a separating, optimal, hyper plane with largest margin. Finding such an optimal separating hyperplane can be shown to be equivalent to minimising the $|\mathbf{w}|$. This can be formulated as follows:

$$
\begin{aligned}
\underbrace{\begin{aligned}
\mathbf{x}_i.\mathbf{w} + b &\geq +1 \quad for \; y_i = +1 \\
\mathbf{x}_i.\mathbf{w} + b &\leq -1 \quad for \; y_i = -1
\end{aligned}} \\
\Downarrow \\
y_i(\mathbf{x}_i.\mathbf{w} + b) - 1 \geq 0 \quad \forall_i
\end{aligned}
\tag{A.1.2}
$$

The distance from the support vectors to the separating hyperplane will be given by $1/|\mathbf{w}|$. The total margin of separation between the two classes will be twice this

distance $2/|\mathbf{w}|$. The aim is to maximise the margin of separation. Since this is given by $2/|\mathbf{w}|$, it is clear that this is equivalent to minimization of the function subject to the constraints $y_i(\mathbf{x}_i.\mathbf{w} + b) \geq 1 \quad \forall_i$.

The constraint equations A.1.2 are multiplied by positive Lagrange multipliers $\alpha_i, i = 1, ..., l$ and subtracted from the objective function. This gives:

$$L_p \equiv \frac{1}{2}||\mathbf{w}||^2 - \sum_{i=1}^{l} \alpha_i y_i(\mathbf{x}_i.\mathbf{w}) + b + \sum_{i=1}^{l} \alpha_i \qquad (A.1.3)$$

We want to minimize L_p with respect to $\mathbf{w}$, b and maximize with respect to all the α_i. Now it is a convex quadratic programming problem. The gradient of L_p with respect to $\mathbf{w}$ and b gives:

$$\mathbf{w} = \sum_i \alpha_i y_i \mathbf{x}_i \qquad (A.1.4)$$

$$\sum_i \alpha_i y_i = 0 \qquad (A.1.5)$$

These are the equality constraints in the dual formulation, we substitute them into equation A.1.3 and it gives:

$$L_D = \sum_i \alpha_i - \frac{1}{2} \sum_{i,j} \alpha_i \alpha_j y_i y_j \mathbf{x}_i.\mathbf{x}_j \qquad (A.1.6)$$

Support vector training maximizes L_D with respect to the α_i subject to constraints A.1.5 with solution given by A.1.4. Those points for which $\alpha_i > 0$ lying on one of the separating hyper planes H1 or H2, are called the support vectors. The support vectors are the critical elements of the training set. They lie closest to the decision boundary; if all other training points were removed and training was repeated, the same separating hyperplane would be found.

The class label (positive or negative) of a new data point x is assigned by using the **decision function** is generalized from equation A.1.4 such that :

$$F(x) = sign(\mathbf{w}.x + b) = sign(\sum_{i=1}^{Ns} \alpha_i y_i(\mathbf{x}_i.x) + b) \qquad (A.1.7)$$

where y_i are the class labels; (.) indicates the inner product; b is the bias; N_s are the set of support vectors; α_i are the positive Lagrange multipliers.

A.2 The non-separable case

The equation A.1.2 cannot find a feasible solution for the linear non-separable case because of the objective function (i.e. L_D) growing arbitrarily large. In order to take good results, additional slack variables $\xi_i, i = 1, ..., l$ are introduced and the equation A.1.2 becomes as follows:

$$
\begin{aligned}
\mathbf{x}_i.\mathbf{w} + b &\geq +1 - \xi_i \quad for\ y_i = +1 \\
\mathbf{x}_i.\mathbf{w} + b &\leq -1 + \xi_i \quad for\ y_i = -1 \\
\xi_i &\geq 0 \quad \forall_i
\end{aligned}
\tag{A.2.8}
$$

Thus, if an error occurs, the corresponding ξ_i must exceed unity; so, $\sum_i \xi_i$ is the upper bound on the number of training errors. Hence, an extra cost for errors to change the objective function to be minimized from $2/|\mathbf{w}|$ to $2/|\mathbf{w}| + C(\sum_i \xi_i)^k$, where C is a **regularization parameter** which is used to balance the complexity of the machine with the number of misclassified points (a larger C corresponding to assign the higher penalty to errors).

The problem again turns to a convex programming problem. As before, by adding the Lagrange multipliers, the dual problem becomes maximise:

$$
L_D = \sum_i \alpha_i - \frac{1}{2} \sum_{i,j} \alpha_i \alpha_j y_i y_j \mathbf{x}_i.\mathbf{x}_j
\tag{A.2.9}
$$

subject to constraints:

$$
\begin{aligned}
0 &\leq \alpha_i \leq C \\
\sum_i \alpha_i y_i &= 0
\end{aligned}
\tag{A.2.10}
$$

The solution of L_D equation A.2.9 is given by :

$$
\mathbf{w} = \sum_i^{Ns} \alpha_i y_i \mathbf{x}_i
\tag{A.2.11}
$$

where N_s is the number of support vectors. The difference from the optimal hyper plane case is that the α_i have an upper bound of C. The non-separable case is depicted in Figure A.3.
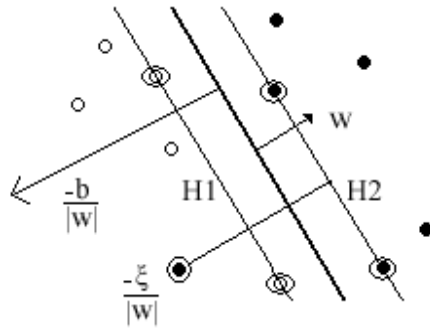
Figure A.3: Linear separating hyperplanes for the non-separable case.

In the case of **linearly non-separable** data, one can use different **kernel functions** to obtain better separation with linear hyper planes. The most commonly used kernel functions are listed below:

$$
\begin{aligned}
Polynomial \quad &: \quad K(x,y) = ((x.y) + \theta)^d \\
Gaussian \quad &: \quad K(x,y) = exp(-\frac{||x-y||^2}{2\sigma^2}) \\
Sigmoid \quad &: \quad K(x,y) = tanh((x.y) + \theta)
\end{aligned}
$$

Appendix B

Hidden Markov Models

HMMs are good at capturing the temporal nature of a process such as speech and they are well suited for problems with a simple grammatical structure. This review is formed using Rabiner's tutorial [69].

If we would have a sequence of observations (discrete or continuous), we can build a signal model that characterizes the occurrence of the observed symbols. After building this signal model, we could recognize other given sequence of observations.

Assume that a system that is described at any time being in one of the **N** states (as depicted in Figure B.1). The current state is update by another state according to probabilities associated with states. The full probabilistic description of such a system requires the description of current and previous states at time t and t-1, respectively. However, for the discrete case, only current and previous states are specified as below.

$$P[q_t = S_i | q_{t-1} = S_j, q_{t-2} = S_k, \cdots] = P[q_t = S_i | q_{t-1} = S_j] \tag{B.0.1}$$

The right side of the equation B.0.1 is independent of time, the state transition probabilities a_{ij} will be:

$$a_{ij} = P[q_t = S_i | q_{t-1} = S_j] \quad 1 \le i, j \le N \tag{B.0.2}$$

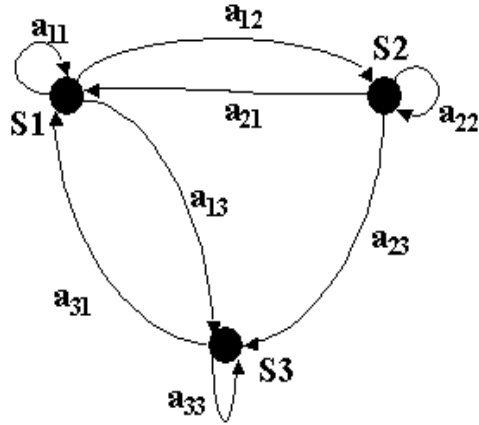$$a_{ij} \ge 0 , \quad \sum_{j=1}^{N} a_{ij} = 1 \tag{B.0.3}$$

Figure B.1: A Markov chain with states (S_1, S_2, S_3) and state transitions $(a_{11}, a_{23}, ...)$.

This system is called **Markov Model**. The output of the model is the state sequences at each time interval and each state corresponds to an event. However, this model is restrictive to apply for many problems. It is extended to the Hidden Markov Model which includes that an observation is a probabilistic function of a state. In that model, the underlying stochastic process is not observable, it can be observable through another set of stochastic process that produce the sequence of observations [69].

B.1   Elements of HMMs

The main elements of an HMM are given as:

1. N is the total number of states in the model. An observation should have a distinctive property within a state.

2. At each time, t, a new state is entered based on the transition probability of the previous state.

3. After each transition is made, an observation symbol is produced according to the emission probability of the current state. The emission probability of each state is independent of the time intervals and previous states.

The notations for common HMMs are described as follows:

- N = number of states in the model

- M = number of distinct observation symbols

- T = length of the observation sequence

- Q = $\{q_1, q_2, \cdots, q_N\}$ states

- V = $\{v_1, v_2, \cdots, v_M\}$ discrete set of possible observation symbols

- A = $\{a_{ij}\}, a_{ij} = P(q_j \ at \ t+1 \mid q_i \ at \ t)$ state transition probability which is the probability of being in state j at time t+1 given that it was in state i at time t.

- B = $\{b_j(k)\}, b_j(k) = P(v_k \ at \ t \mid q_j \ at \ t)$ observation (emission) symbol probability which is the probability of observing the symbol v_k given that in state j.

- $\pi = \{\pi_i\}, \pi_i = P(q_i \ at \ t = 1)$, initial state distribution which is the probability of being in state i at the beginning at time t = 1.

- O_t denotes the observation symbol observed at time t.

Using the HMM an observation sequence O = $O_1, O_2, \cdots, O_T$, is generated as follows: Choose an initial state, i_1 according to the initial state probability π_i, set the time t=1, and choose an observation symbol O_1 according to emission probability distribution $b_i(k)$. After t becomes t+1, choose i_{t+1} according to transition probability distribution a_{t+1} and select observation symbol O_{t+1} according to emission probability distribution $b_j(k)$. Continue this procedure until reach time T.

The compact notation to represent an HMM is $\lambda = (A, B, \pi)$.

B.2   The Three Problems for HMMs

There exist three crucial problems which must be solved for an HMM to use it in applications.

1. **Problem :** Given the model $\lambda = (A, B, \pi)$ how do we compute $P(O|\lambda)$ that is the probability of occurrence of the observation sequence O = $O_1, O_2, \cdots, O_T$.

Another explanation of first problem is that there is a given model and a sequence of observations, so how we evaluate the model.

2. **Problem :** Given the model $\lambda = (A, B, \pi)$ how do we choose a state sequence $I = i_1, i_2, \cdots, i_T$, so that $P(O, I|\lambda)$, the joint probability of the observation sequence $(O = O_1, O_2, \cdots, O_T,)$ and state sequence (I) given the model (λ) is maximized. That problem tries to find the hidden part of a model, state sequence.

3. **Problem :** How we could adjust the HMM parameters $\lambda = (A, B, \pi)$ so that $P(O|\lambda)$ is maximized. It optimizes the model parameters to describe the observation sequence. These parameters are used in the training of the model.

B.2.1 Solution to the First Problem

The aim is to calculate the probability of the observation sequence given the model. The easiest way of doing that to enumerate every possible state sequence. For a fixed state sequence $I = i_1, i_2, \cdots, i_T,$, the probability of the observation sequence O is:

$$P(O|I, \lambda) = b_{i_1}(O_1)b_{i_2}(O_2)\cdots b_{i_T}(O_T) \tag{B.2.4}$$

The probability of a state sequence I is:

$$P(I|\lambda) = \pi_{i_1}a_{i_1 i_2}a_{i_2 i_3}\cdots a_{i_{T-1} i_T} \tag{B.2.5}$$

The joint probability of O and I is the multiplication of the probabilities in equations B.2.4 and B.2.5.

$$P(O, I|\lambda) = P(O|I, \lambda)\,P(I|\lambda) \tag{B.2.6}$$

The probability of O that given model λ can be calculated using summation of the joint probability $(P(O, I|\lambda))$ over all possible state sequences (I) :

$$P(O|\lambda) = \sum_I P(O|I, \lambda)P(I|\lambda) = \sum_{i_1, i_2, \ldots, i_T} \pi_{i_1} b_{i_1}(O_1)a_{i_1 i_2}b_{i_2}(O_2)\cdots a_{i_{T-1} i_T}b_{i_T}(O_T)$$
$$\tag{B.2.7}$$

74

In equation B.2.7, the multiplications require 2T-1 computations. All possible state sequences are N^T. So, it requires the $2\text{T}.N^T$ multiplications, it is hugh computations. Therefore, another method, **forward-backward procedures**, was developed to solve this problem.

B.2.1.1   Forward Procedure

Assume that a **forward variable** $\alpha_t(i)$ is defined as follows:

$$\alpha_t(i) = P(O_1, O_2, \cdots, O_T, i_t = q_i | \lambda) \tag{B.2.8}$$

The probability of the partial observation sequence up to time t and the state q_i at time t given the model λ. The $\alpha_t(i)$ is computed as follows:

1. Initialization:

$$\alpha_t(i) = \pi_i . b_i(O_1) \; ; \qquad 1 \leq i \leq N \tag{B.2.9}$$

   It initiates the forward probabilities as the joint probability of state q_i and initial observation O_1.

2. Induction:

$$\text{for } t = 1, 2, \cdots, T-1 \; ; \quad 1 \leq j \leq N$$

$$\alpha_{t+1}(j) = \left[\sum_{i=1}^{N} \alpha_i a_{ij} \right] b_j(O_{t+1}) \tag{B.2.10}$$

   Figure B.2 depicts that how state q_j is reached at time t+1 from N possible of states, q_i, at time t. The $\alpha_t(i)$ is the probability of joint event $(O_1, O_2, \cdots, O_t)$ and states q_i stops at time t. The product of $\alpha_i a_{ij}$ is the probability of the joint event $(O_1, O_2, \cdots, O_t)$ and state q_j reaches at time t+1. The summation of this product over all possible N states for q_i includes previous observations. After that computation is performed and S_j is known, the $\alpha_{t+1}(j)$ is computed by multiplying the summed quantity with the emission probability $b_j(O_{t+1})$.

3. Termination

$$P(O|\lambda) = \sum_{i=1}^{N} \alpha_T(i) \qquad \text{(B.2.11)}$$

It gives the calculation of $P(O|\lambda)$ as the summation of the forward variables $\alpha_T(i)$.

The total calculations requiring for the $\alpha_{t+1}(j)$ are order of N^2T not $2TN^T$. Hence, the forward procedure is saving a hugh amount of computations.
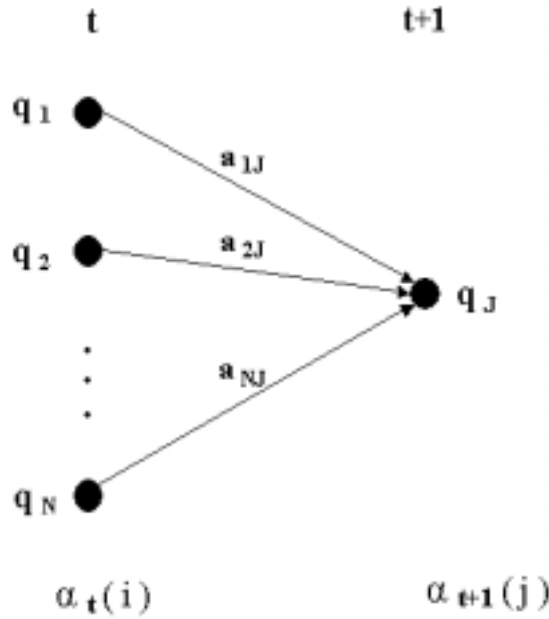

Figure B.2: Illustration of the stages required for the computation of $\alpha_{t+1}(j)$.

B.2.1.2   Backward Procedure

In the similar way, a **backward variable** $\beta_t(i)$ is defined as follows:

$$\beta_t(i) = P(O_{t+1}, O_{t+2}, \cdots, O_T, i_t = q_i, \lambda) \qquad \text{(B.2.12)}$$

The probability of the partial observation sequence from time t+1 to end, the state q_i at time t given the model λ. The $\beta_t(i)$ is computed as follows:

1. Initialization :

$$\beta_t(i) = 1 ; \qquad 1 \le i \le N \qquad \text{(B.2.13)}$$

It defines the backward probabilities 1 for all i.

2. Induction :

$$for\ t = T - 1, T - 2, \cdots, 1 ; \quad 1 \leq j \leq N$$

$$\beta_t(i) = \sum_{j=1}^{N} a_{ij} b_j O_{(t+1)} \beta_{t+1}(j) \tag{B.2.14}$$

Figure B.3 depicts that being in state q_i at time t, must be calculated the rest of the observation sequence $(\beta_{t+1}(j))$, transitions to every one of the N states at time t+1 (a_{ij} term), the observation O_{t+1} in state j ($b_j O_{(t+1)}$ term).
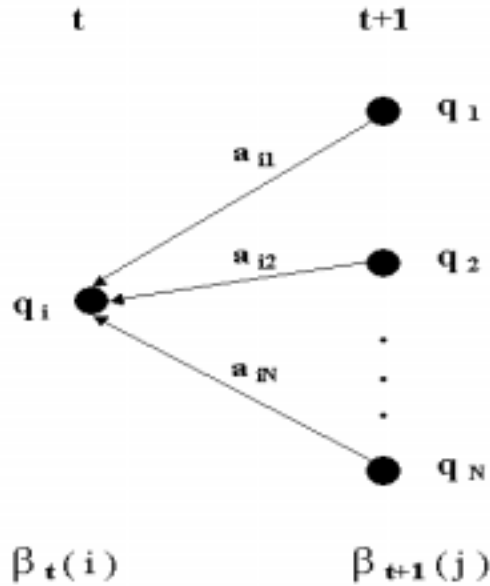
Figure B.3: Illustration of the stages required for the computation of $\beta_t(i)$.

The total calculations requiring for the $\beta_t(i)$ are also order of $N^2 T$. Hence, both of forward and backward procedures are equally efficient to compute the $P(O|\lambda)$.

B.2.2 Solution to the Second Problem

There are several ways to solve the second problem that is finding the optimal state sequence associated with the observation sequence. The famous method is called **Viterbi Algorithm**.

B.2.2.1 Viterbi Algorithm

It is an inductive algorithm, a kind of dynamic algorithm, at each instant the best (with maximum probability) possible state sequence is kept. In this way we finally have the best path for each of N states as the last state for the desired observation sequence. Then we choose the one with the highest probability.

In order to find best state sequence (Q $=q_1 q_2 \cdots q_t$) for the given observation sequence (O $=O_1 O_2 \cdots O_T$), a quantity is defined: $\delta_t(i)$ is the best score along a single path, it accounts for the first t observation and stops in state q_i. The definition of $\delta_t(i)$ is:

$$\delta_t(i) = \max_{q_1 q_2 \cdots q_{t-1}} P[q_1 q_2 \cdots q_t = i, O_1 O_2 \cdots O_T | \lambda] \qquad \text{(B.2.15)}$$

We calculate $\delta_{t+1}(j)$ by induction such as:

$$\delta_{t+1}(j) = [\max_i \delta_t(i) a_{ij}] b_j(O_{t+1}) \qquad \text{(B.2.16)}$$

We should keep the track of the argument maximized (eq. B.2.16) for each t and j, to retrieve the state sequence later. The storage $\psi_t(j)$ is used for that purpose. The formal steps to find the best state sequence are given below :

1. Initialization :
$$\delta_1(i) = \pi_i b_i(O_1) \quad 1 \leq i \leq N$$
$$\psi_1(i) = 0 \qquad \text{(B.2.17)}$$

2. Recursion :

$$\delta_t(j) = \max_{1 \leq i \leq N} [\delta_{t-1}(i) a_{ij}] \, b_j(O_t) \qquad 2 \leq t \leq T; \;\; 1 \leq j \leq N \qquad \text{(B.2.18)}$$

$$\psi_t(j) = arg \max_{1 \leq i \leq N} [\delta_{t-1}(i) a_{ij}] \qquad 2 \leq t \leq T; \;\; 1 \leq j \leq N \qquad \text{(B.2.19)}$$

3. Termination :

$$P^* = \max_{1 \leq i \leq N} [\delta_T(i)] \qquad \text{(B.2.20)}$$

$$q_T^* = arg \max_{1 \leq i \leq N} [\delta_T(i)] \qquad \text{(B.2.21)}$$

4. State sequence backtracking :

$$q_t^* = \psi_{t+1}(q_{t+1}^*) \qquad t = T-1, T-2, \cdots, 1 \qquad \text{(B.2.22)}$$

The Viterbi algorithm is very similar to forward-backward procedure except for the comparisons required to find the maximum value. The complexity of Viterbi algorithm is also the order of $N^2 T$.

B.2.3   Solution to the Third Problem

The last problem deals with the determination of the model training parameters. It optimizes the model parameters (A, B, π) to make the maximum the probability of observation sequence. We will choose these parameters (A, B, π) using an iterative process such as **Baum-Welch** method.

B.2.3.1   Baum-Welch Algorithm

It adjusts the model parameters to increase $P(O|\lambda)$. The calculation of $P(O|\lambda)$ is the summation of $P(O, I|\lambda)$ over all possible state sequence (I). However, we should make this optimization for all states sequences not a given one to solve the third problem.

Baum-Welch Algorithm takes an initial model that is improved until $P(O|\lambda)$ becomes maximum. So, we assume that there is an initial HMM at the beginning. Then a probability, $\xi_t(i,j)$, is defined as:

$$\xi_t(i,j) = P[i_t = q_t | i_{t+1} = q_j | O, \lambda] \qquad \text{(B.2.23)}$$

It is the probability of a being in state q_i at time t and going to state q_j at time t+1, given the observation sequence (O) and model (λ). By using equations in forward-backward procedures, $\xi_t(i,j)$ is written as :

$$\xi_t(i,j) = \frac{\alpha_t(i) \; a_{ij} \; b_j \; (O_{t+1}) \; \beta_{t+1}(j)}{P[O|\lambda]} \qquad \text{(B.2.24)}$$

where $\alpha_t(i)$ accounts for the observations $O_1, O_2, \cdots, O_t$; a_{ij} accounts for the transition to state j; $b_j\,(O_{t+1})$ picks up the symbol O_{t+1} from state j; $\beta_{t+1}(j)$ accounts for the remaining observation sequences $O_{t+2}, O_{t+3}, \cdots, O_T$.

Now, we define a new variable, $\gamma_t(i)$, which is the probability of being state q_i at time t, given the observation sequence and the model:

$$\gamma_t(i) = P(i_t = qi|O, \lambda) \tag{B.2.25}$$

Using Bayes law and forward-backward procedure, $\gamma_t(i)$ can be written as:

$$\gamma_t(i) = \frac{P(i_t = qi, O|\lambda)}{P(O|\lambda)} = \frac{\alpha_t(i)\,\beta_t(i)}{P(O|\lambda)} \tag{B.2.26}$$

If we consider the equations B.2.24 and B.2.26, the summation of $\xi_t(i,j)$ over all j gives the $\gamma_t(i)$ as follows:

$$\gamma_t(i) = \sum_{j=1}^{N} \xi_t(i,j) \tag{B.2.27}$$

The summation of $\gamma_t(i)$ from $t = 1\ to\ T$ gives the expected number of times that state q_i is visited. Similarity, the summation of $\gamma_t(i)$ from $t = 1\ to\ T-1$ gives the expected number of transitions made from state q_i. The summation of $\xi_t(i,j)$ from $t = 1\ to\ T-1$ gives the expected number of transitions from state q_i to q_j. So,

$$\sum_{t=1}^{T-1} \gamma_t(i) = Expected\ number\ of\ transitions\ made\ from\ state\ q_i \tag{B.2.28}$$

$$\sum_{t=1}^{T-1} \xi_t(i,j) = Expected\ number\ of\ transitions\ from\ state\ q_i\ to\ q_j \tag{B.2.29}$$

The Baum-Welch re-estimation formulas are presented using above equations:

$$\bar{\pi}_i = \gamma_1(i) \tag{B.2.30}$$

$$\bar{a}_{ij} = \sum_{t=1}^{T-1} \xi_t(i,j) \Bigg/ \sum_{t=1}^{T-1} \gamma_t(i) \tag{B.2.31}$$

$$\bar{b_j}(k) = \sum_{\substack{t=1 \\ O_t=k}}^{T} \gamma_t(j) \Bigg/ \sum_{t=1}^{T} \gamma_t(j) \tag{B.2.32}$$

The re-estimation formula for π_i is the probability of being in state q_i at time t=1. The formula for a_{ij} is the ratio of expected number of making transitions from state q_i to state q_j divided by the expected number of making transitions out of state q_i. The formula for $b_j(k)$ is the ratio of the expected number of times of being in state q_j, observing symbol O_k divided by the expected number of times being in state q_j. The summation for $b_j(k)$ goes from t=1 up to t=T.

The initial model is λ and the re-estimation model is $\bar{\lambda}$ which consists of the above parameters $\bar{\pi}_i$, $\bar{a}_{ij}$, $\bar{b}_j(k)$, then it can be shown that either :

1. The initial model λ is a critical point of the likelihood function in which case $\bar{\lambda} = \lambda$ or,

2. $P(O|\bar{\lambda}) > P(O|\lambda)$, found a better model $\bar{\lambda}$ from which the observation sequence is more likely to be produced.

If $\bar{\lambda}$ is used in place of λ iteratively and repeated the re-estimation, we could improve the probability of O being observed form the model. The final result of the re-estimation operation is called maximum likelihood estimate of the HMM.

Appendix C

Artificial Neural Networks

The neurons are found in the human brain that are many and varied. Artificial neurons are simplified models based on the known properties of biological neurons. The Artificial Neural Network (ANN) is a parallel dynamical system consisting of multiple simple units that can perform transformations by their state response to their input information.

Over the last decade, many different ANN models have been proposed for broad range of applications. For supervised classification tasks, the multilayer feedforward neural network (MLP) and the learning vector quantisation (LVQ) network are the most commonly used models.

The multi-layer perceptron came into favor when Rumelhart et.al. applied the gradient backpropagation algorithm for training layered networks of perceptron elements [78]. The LVQ method was developed by Kohonen who also developed the popular unsupervised classification technique known as the self-organising map neural networks [47].

C.1 The Artificial Neuron

An artificial neuron computes a function of a weighted sum of inputs:

$$y = f(a) = f(\sum_{i}^{n} x_i w_i - b) \qquad (C.1.1)$$

where x_i input, each input has an associated w_i weight, **b** is a threshold value to be activated or not. The illustration of a neuron is given in Figure C.1.
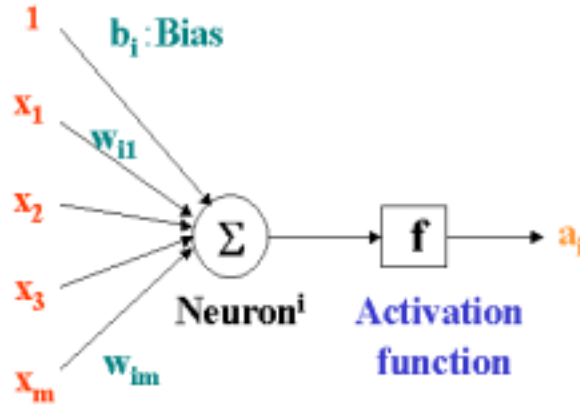
Figure C.1: The architecture of one neuron.

There are several number of variations on the activation function used in ANNs. The most commons are listed in Table C.1.

Name	Input/Output Relation
Linear	$a = n$
Threshold	$a = 0, n < 0$ $a = 1, n \geq 0$
Symmetrical Threshold	$a = -1, n < 0$ $a = 1, n \geq 0$
Positive Linear	$a = 0, n < 0$ $a = n, n \geq 0$
Sigmoid	$a = \frac{1}{1+e^{-n}}$
Tangent Sigmoid	$a = \frac{e^n - e^{-n}}{e^n + e^{-n}}$

Table C.1: Several different activation functions.

Sigmoidal functions provide a smooth, continuous version of threshold function, which are differentiable. Sigmoidal units are also able to incorporate a threshold or bias value, that effectively translates the center of the sigmoid to some arbitrary value.

C.2 Multilayer Perceptrons

The most widely used neural classifier today is Multilayer Perceptron (MLP). The MLP belongs to the class of supervised neural networks. MLPs are general-purpose, flexible, non-linear models consisting of a number of neurons organised into multiple layers. The complexity of the MLP can be changed by varying the number of layers and the number of neurons in each layer. Given enough hidden neurons and enough

data, MLPs can approximate virtually any function to any desired accuracy. MLPs are valuable tools in problems when one has little or no knowledge about the form of the relationship between input vectors and their corresponding outputs.

The MLP consists of a network of processing elements or neurons arranged in layers. It requires three or more layers of processing neurons: an input layer which accepts the input variables used in the classification procedure, one or more hidden layers, and an output layer with one neuron per class. The principle of the network is that when data from an input pattern is presented at the input layer, the network neurons perform calculations in the successive layers until an output value is computed at each of the output neurons. This output signal should indicate which is the appropriate class for the input data (a high output value on the correct class neuron and a low output value on all the rest). The connections between neurons are undirectional, it means that there is no feedback or cycles in the network. The connections carry weights which encapsulate the behaviour of the network and are adjusted during training. A MLP is said to be **fully connected** if every neuron in a given layer is connected to every neuron in the following layer. The architecture of a 3 layer fully connected MLP is illustrated in Figure C.2.
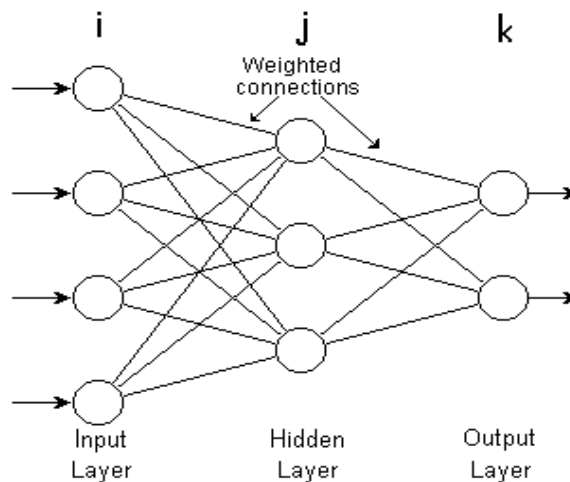

Figure C.2: The architecture of 3 layer fully connected MLP.

The operation of MLP consists of two stages, the **forward pass** and the **backward pass** or **backpropagation**. In the forward pass an input pattern vector is presented to the network and the output of the input layer neurons is the components of the input pattern. In the hidden layers, the input for each neuron is the

sum of the scalar products of the incoming vector components with their respective weights. The input of a neuron j is given by:

$$input_j = \sum_i^n w_{ji} out_i \qquad (C.2.2)$$

where w_{ji} is the weight connecting neuron i to neuron j and out_i is the output of neuron i. The output of neuron j is given by:

$$out_j = f(input_j) \qquad (C.2.3)$$

The function **f** denotes the activation function of each neuron. The output of a neuron is sent to all neurons in the following layer. It will continue through all the layers until the output layer is reached. The input layer neurons just take the corresponding value from the input pattern vector.

The MLP is trained by supervised learning using the iterative backpropagation algorithm. In the learning phase, the training set patterns are presented at the input layer as feature vectors, together with their corresponding desired output (target) pattern which represents the classification for the input pattern. The training starts with small random weights. For each input pattern the network is required to adjust the weights attached to the connections so that the difference between the network's output and the target for that input pattern is decreased. The weights between the output layer and the below hidden layer are adjusted by the generalised delta rule [78]:

$$w_{kj}(t+1) = w_{kj}(t) + \eta(\delta_k \; out_k) \qquad (C.2.4)$$

where $w_{kj}(t+1)$ and $w_{kj}(t)$ are the weights connecting neurons j and k at iteration (t+1) and t, respectively, η is a learning rate parameter. The δ for the hidden layer neurons are calculated and the weights connecting the hidden layer with the layer below are updated. This procedure is repeated until the last layer of weights has been adjusted. Section C.2.1 shows how the generalised delta rule and δ are derived.

C.2.1   Backpropagation Algorithm

The backpropagation algorithm is a gradient descent optimisation procedure which minimises the **mean square error** between the network's output and the target for all input patterns **N**.

$$E = \frac{1}{2N} \sum_p \sum_k (target_k - out_k)^2 \qquad (C.2.5)$$

The training set is presented iteratively to the network until a stable set of weights is achieved and the error function is reduced to an acceptable level. It is done by a series of **gradient descent** weight updates:

$$\Delta w_{kj} = -\eta \frac{\partial E_p}{\partial w_{kj}} \qquad (C.2.6)$$

where E_p is the mean squared error for input pattern p and is given by:

$$E_p = \frac{1}{2} \sum_p (target_k - out_k)^2 \qquad (C.2.7)$$

Using the chain rule the right hand side term of equation C.2.6 can be written as follows:

$$-\frac{\partial E_p}{\partial w_{kj}} = -\frac{\partial E_p}{\partial\ input_k} \frac{\partial\ input_k}{\partial w_{kj}} \qquad (C.2.8)$$

The weight changes can be expressed as the product of two terms; the rate of change of error with respect to the input to neuron k and the change of the input to neuron k with respect to a change in the weight between neurons j and k. If we apply the equation C.2.2 to the second part of equation C.2.8 :

$$\frac{\partial\ input_k}{\partial w_{kj}} = \frac{\partial \sum w_{kj} out_j}{\partial w_{kj}} = out_j \qquad (C.2.9)$$

We define δ_k as :

$$\delta_k = -\frac{\partial E_p}{\partial\ input_k} \qquad (C.2.10)$$

We substitute the equations C.2.9 and C.2.10 in equation C.2.6 :

$$\Delta w_{kj} = -\eta \delta_k out_j \qquad (C.2.11)$$

86

If we use the chain rule, we can express δ_k in terms of the rate of change of error with respect to the output of neuron k and the change of the output of neuron k with respect to the input to the neuron k as follows:

$$\delta_k = -\frac{\partial E_p}{\partial\ input_k} = -\frac{\partial E_p}{\partial out_k}\ \frac{\partial out_k}{\partial\ input_k} \qquad (C.2.12)$$

Using equation C.2.3 we get :

$$\frac{\partial out_k}{\partial\ input_k} = f'(input_k) \qquad (C.2.13)$$

Using equation C.2.7 we get :

$$\frac{\partial E_p}{\partial out_k} = -(target_k - out_k) \qquad (C.2.14)$$

When we substitute the equations C.2.13 and C.2.14 in equation C.2.10, we get the δ for an output neuron k as follows:

$$\delta_k = (target_k - out_k)\ f'(input_k) \qquad (C.2.15)$$

Finally if we substitute equation C.2.15 in equation C.2.11, we get:

$$\Delta w_{kj} = -\eta\ (target_k - out_k)\ f'(input_k)\ out_j \qquad (C.2.16)$$

If we have a neuron j which is in the hidden layer, we use chain rule to get δ_j :

$$\delta_j = f'(input_j) \sum_k \delta_k w_{kj} \qquad (C.2.17)$$

The weight update of that neuron j will be :

$$\Delta w_{ji} = -\eta\ f'(input_j) \sum_k \delta_k w_{kj}\ out_i \qquad (C.2.18)$$

The equations C.2.18 and C.2.16 are the weight update rules for the hidden and the output layers, respectively.

If we update the weights after each training pattern, rather than adding up the weight changes for all the patterns before applying them, the learning algorithm is

no longer true gradient descent. It is called **online learning**. If we keep the step sizes (η) small enough, the erratic behaviour of the weight updates will not be too much of a problem, and the increased number of weight changes will still get us to the minimum quicker than true gradient descent. It is called **batch learning**.

The training steps of a fully connected MLP is given below:

1. Take the set of N training patterns to learn

2. Set up the network with **i** input units fully connected to **j** hidden units via connections with weights w_{ji}, which in turn are fully connected to **k** output units via connections with weights w_{kj}

3. Generate random initial weights

4. Select an appropriate error function $E(w_{kj})$ and learning rate η

5. Apply the weight update equation $\Delta w_{kj} = -\eta \frac{\partial E(w_{kj})}{\partial w_{kj}}$ to each weight w_{kj} for each training pattern p. One set of updates of all the weights for all the training patterns is called one epoch of training

6. Repeat step 5 until the network error function is small enough.

C.3 Heuristics for MLPs

Several number of heuristics are developed to use in training a MLP. Some of them are widely considered to be very useful for improving the training speed and quality of solution reached by training algorithms.

1. Initialization of weight values: The weights in a MLP should be initialized to small, random values prior to training. The performance of backpropagation and other algorithms can be highly dependent on the initialization of weights. The general heuristic commonly used is to initialize weights such that the sigmoidal activation functions in the network operate in their linear range (very small weights however result in very small gradient values).

2. Pre-processing of training data: The pre-processing includes the dimensionality reduction techniques which attempt to reduce the number of inputs without

losing information relevant for training. One method includes the removal of any biases in the inputs by translating such that their mean values are close to zero and their variances are similar to each other. Another step is to remove correlations between inputs.

3. Learning rate: Standard backpropagation uses a single learning rate parameter. The value of the learning rate is problem dependent and is usually set by experiments during training. This parameter constrains the step sizes that are taken in each component direction in weight space through the multiplication with a common constant. Principled methods exist for computing the single optimal learning rate for backpropagation and optimal learning rates for each weight, using Hessian information during training.

4. Momentum: By adding a new parameter we can smooth out the erratic behaviour of the online updates, to update the weights with the moving average of the individual weight changes corresponding to a single training pattern. If we label everything by the time t, the implementing a moving average will be:

$$\Delta w_{ji}(t+1) = -\eta \sum_p \delta_i(t+1) \, out_j(t+1) + \alpha \, \Delta w_{ji}(t) \qquad \text{(C.3.19)}$$

We add a **momentum** term $\alpha \, \Delta w_{ji}(t)$ which is the weight change of the previous step times a momentum parameter α. If α is zero, then we have the standard online training algorithm used before. If we increase α towards one, each step includes increasing contributions from previous training patterns. It makes no sense to have α less than zero or greater than one. Good sizes of α depend on the size of the training data set. Usually, we will need to decrease η as we increase α so that the total step sizes do not get too large.

Bibliography

[1] Altschul, S., Madden, T., Shaffer, A., Zhang, J., Zhang, Z. Gapped Blast and PSI-Blast: a new generation of protein database search programs. Nucl. Acids Res. 25, 3389-3402, 1997

[2] Bahar, I., Atilgan, A. R., Jernigan, R. L., Erman, B. Understanding the recognition of protein structural classes by amino acid composition. Proteins, 29(2), 172-185, 1997

[3] Baldi, P., Brunak, S., Frasconi, P., Soda, G., Pollastri, G. Exploiting the past and the future in protein secondary structure prediction. Bioinformatics, 15, 937-946, 1999

[4] Baysal, C., Atilgan, A. R. Coordination Topology and Stability for the Native and Binding Conformers of Chymotrypsin Inhibitor 2. Proteins, 45, 62-70, 2001

[5] Berman, H. M., Westbrook, J., Feng, Z., Gilliland, G., Bhat, T. N., Weissig, H., Shindyalov, I. N., Bourne, P. E. The Protein Data Bank. Nucleic Acids Res. 28(1), 235-242, 2000

[6] Blout, E. R. The dependence of the conformation of polypeptides and proteins upon amino acid composition. Polyamino Acids, Polypeptides, and Proteins, 275-279, 1962

[7] Bryant, S.H. Evaluation of threading specificity and accuracy. Proteins: Struct. Funct. Genet. 26, 172-185, 1996

[8] Burges, C.J. C. A Tutorial on Support Vector Machines for Pattern Recognition. Data Mining and Knowledge Discovery, 2, 121-167, 1998

[9] Cai, Y., Zhou, G. Prediction of protein structural classes by neural network. Biochem. 82(8), 783-787, 2000

[10] Cai, Y. D., Liu, X. J., Xu, Xb., Chou, K. C. Prediction of protein structural classes by Support Vector Machines. Comput. Chem. 26(3), 293-296, 2002

[11] Cai, D. Y., Liu X. J., Xu, X. B., Chou, K. C. Support Vector Machines for the classification and prediction of β-turn types. J. Pept. Sci. 8, 297-301, 2002

[12] Chandonia, J. M., Karplus, M. Neural networks for secondary structure and structural class predictions. Protein Sci. 4(2), 275-285, 1995

[13] Chang, C. C., Lin, C. J. LIBSVM: a Library for Support Vector Machines. Version=2.33, 2002

[14] Chou, K. C. A novel approach to predicting protein structural classes in a (20-1)-D amino acid composition space. Proteins, 21(4), 319-344, 1995

[15] Chou, K. C. Prediction and classification of β-turn types. Biopolymers, 42, 837-853, 1997

[16] Chou, K. C. Prediction of tight turns and their types in proteins. Analy. Biochem. 286, 1-16, 2000

[17] Chou, K. C. A key driving force in determination of protein structural classes. Biochem. Biophys. Res. Commun. 264(1), 216-224, 1999

[18] Chou, P. Y., Fasman, G. D. Prediction of protein conformation. Biochemistry, 13, 222-245, 1974

[19] Chou, P. Y. Prediction of protein structural classes from amino acid composition. Prediction of protein structure and the principles of protein conformation(E. Fasman, G. D.), Plenum Press, New York, 549-586, 1989

[20] Cristianini, N., Scholkopf, B. Support Vector Machines and Kernel Methods, The New Generation of Learning Machines. AI Magazine, 23(3), 31-41, 2002

[21] Cuff, J. A., Barton, G. J. Application of multiple sequence alignment profiles to improve protein secondary structure prediction. Proteins, 40, 502-511, 2000

[22] Deleage, G., Dixon, J.S. Use of class prediction to improve protein secondary structure prediction. Prediction of protein structure and the principles of protein conformation (E. Fasman, G. D.), Plenum Press, New York, 587-597, 1989

[23] Di Francesco, V., Garnier, J., Munson, P. J. Improving protein secondary structure prediction with aligned homologous sequences. Prot. Sci. 5, 106-113, 1996

[24] Ding, C. H., Dubchak, I. Multi-class protein fold recognition using support vector machines and neural networks. Bioinformatics, 17(4), 349-358, 2001

[25] Eddy, S. R. Profile hidden Markov models. Bioinformatics,14, 755-763, 1998

[26] Eisenhaber, F., Persson, B., Argos, P. Protein structure prediction: recognition of primary, secondary, and tertiary structural features from amino acid sequence. Crit. Rev. Biochem. Mol. Biol. 30(1), 1-94, 1995

[27] Frishman, D., Argos, P. 75% accuracy in protein secondary structure prediction. Proteins, 27, 329-335, 1997

[28] ftp://ftp.embl-heidelberg.de/pub/databases/protein_extras/pdb_select

[29] Higgins, D. G., Thompson, J. D., Gibson, T. J. Using CLUSTAL for multiple sequence alignments. Meth. Enzymol. 266, 383-402, 1996

[30] Hobohm, U., Sander, C. Enlarged representative set of protein structures. Protein Sci. 3, 522, 1994

[31] Holley, H., Karplus, M. Protein secondary structure prediction with a neural network. Proceedings of the National Academy of Science of the United States of America, 86, 152-156, 1989

[32] http://htk.eng.cam.ac.uk/

[33] Hughey, R., Krogh, A. Hidden Markov models for sequence analysis: extension and analysis of the basic method. CABIOS, 12, 95-107, 1996

[34] Hutchinson, E. G., Thornton, J. M. A revised set of potentials for β-turn formation in proteins. Protein Sci. 3, 22072216, 1994

[35] Hutchinson, E. G. and Thornton, J. M. PROMOTIF - a program to identify and analyze structural motifs in proteins. Protein Sci. 5, 212-220, 1996

[36] Islamaj, Rezerta. Two or three dimensional representation of amino acid characteristics. 2000

[37] Jones, D. T., Taylor, W. R., Thornton, J. M. A new approach to protein fold recognition. Nature, 358, 86-89, 1992

[38] Jones, D. T. GenThreader: An efficient and reliable protein fold recognition method for genomic sequences. J. Mol. Biol. 287, 797-815, 1999

[39] Jones, D. T. Protein secondary structure prediction based on position-specific scoring matrices. J. Mol. Biol. 292, 195-202, 1999

[40] Kabsch, W., Sander, C. Dictionary of protein secondary structure: pattern recognition of hydrogen-bonded and geometrical features. Biopolymers, 22(12), 2577-2637, 1983

[41] Karplus, K., Barrett, C., Hughey, R. Hidden Markov models for detecting remote protein homologies. Bioinformatics, 14, 846-856, 1998

[42] Karplus, K., Barrett, C., Cline, M., Diekhans, M., Grate, L. Predicting protein structure using only sequence information. Proteins, S3, 121-125, 1999

[43] Kaur, H., Raghava, G.P.S. Prediction of β-turns in proteins from multiple alignment using neural network. Protein Science, 12, 627-634, 2003

[44] King, R. D., Sternberg, M. J. Identification and application of the concepts important for accurate and reliable protein secondary structure prediction. Prot. Sci. 5, 2298-2310, 1996

[45] Klein, P., Delisi, C. Prediction of protein structural class from the amino acid sequence. Biopolymers, 25(9), 1659-1672, 1986

[46] Kneller, D., Cohen, F. Improvements in secondary structure prediction by an enhanced neural network. J. Mol. Biol. 214, 171-182, 1990

[47] Kohonen, T. Selforganized formation of topologically correct feature maps. Biological Cybernetics, 43, 59-69, 1982

[48] Lathrop, R. H., Smith, T. F. Global optimum protein threading with gapped alignment and empirical pair score functions. J. Mol. Biol. 255, 641-665, 1996

[49] Lehninger, A. L., Nelson, D. L., Cox, M. M. Lehninger Principles of Biochemistry. Third Edition

[50] Leslie, C., Eskin, E., Noble, W. S. The Spectrum Kernel: A String Kernel For SVM Protein Classification. Pacific Symposium on Biocomputing, Hawaii, USA, 2002

[51] Levin, J. M., Pascarella, S., Argos, P., Garnier, J.Quantification of secondary structure prediction improvement using multiple alignment. Prot. Engin. 6, 849-854, 1993

[52] Levitt, M., Chothia, C. Structural patterns in globular proteins. Nature, 261(5561), 552-558, 1976

[53] Lewis, P. N., Momany, F. A., Scheraga, H. A. Chain reversals in proteins. Biochim. Biophys. Acta. 303, 211-229, 1973

[54] Maclin, R., Shalvik, J. Using knowledge-based neural networks to improve algorithms: refining the chou-fasman algorithm for protein folding. Machine Learning, 11, 195-215, 1993

[55] Mahalanobis, P. C. On the generalized distance in statistics. Proc. Natl. Inst. Sci., Plenum Press,India, 2, 49-55, 1936

[56] Marti-Renom, M.A., Stuart, A., Fiser, A., Sanchez, R., Melo, F., Sali, A. Comparative protein structure modeling of genes and genomes. Annu. Rev. Biophys. Biomol. Struct. 29, 291-325, 2000

[57] Maxfield, F. R., Scheraga, H. A. Improvements in the Prediction of Protein Topography by Reduction of Statistical Errors. Biochem. 18, 697-704, 1979

[58] McGregor, M. J., Flores, T. P., Sternberg, M. J. E. Prediction of β-turns in proteins using neural networks. Protein Eng. 2(7), 521-526, 1989

[59] Mehta, P. K., Heringa, J., Argos, P. A simple and fast approach to prediction of protein secondary structure from multiply aligned sequences with accuracy above 70

[60] Metfessel, B. A., Saurugger, P. N., Connelly, D. P., Rich, S. S. Cross-validation of protein structural class prediction using statistical clustering and neural networks. Protein Sci. 2(7), 1171-1182, 1993

[61] Mount, D.W., Bioinformatics and genome analysis, Cold Spring Harbor Press, 1999

[62] Murzin, A. G., Brenner, S. E., Hubbard, T., Chothia, C. SCOP: a structural classification of proteins database for the investigation of sequences and structures. J. Mol. Biol. 247, 536-540, 1995

[63] Nakashima, H., Nishikawa, K., Ooi, T. The folding type of a protein is relevant to the amino acid composition. J. Biochem. 99(1), 153-162, 1986

[64] Orengo, C. A., Taylor, W. R. SSAP: Sequential structure alignment program for protein structure comparison. Meth. Enzymol. 266, 617-635, 1996

[65] Orengo,C.A., Todd, A., Thornton, J.M. From Protein Structure to Function. Curr. Op. in Str. Biol. 9, 374-382, 1999

[66] Pauling, L., Corey, R. B., Branson, H. R. The structure of proteins: Two hydrogen-bonded helical configurations of the polypeptide chain. Proc. Natl. Acad. Sci. U.S.A. 37, 205-234, 1951

[67] Pearl, F. M. G, Lee, D., Bray, J. E., Sillitoe, I., Todd, A. E., Harrison, A. P., Thornton, J. M., Orengo, C. A. Assigning genomic sequences to CATH Nucleic Acids Research. 28(1), 277-282, 2000

[68] Qian, N., Sejnowski, T. Predicting the secondary structure of globular proteins using neural network models. J. Mol. Biol. 202, 865- 884, 1988

[69] Rabiner, L. R., Juang, B. H. An introduction to hidden markov models. IEEE Magazine on Accoustics, Speech and Signal Processing, 3(1), 4-16, 1986

[70] Richardson, J. S. The anatomy and taxonomy of protein structure. Adv. Protein Chem. 34, 167339, 1981

[71] Richardson, J. S. Richardson, D. C., Principles and patterns of protein conformation. Prediction of protein structure and the principles of protein conformation(E. Fasman, G. D.), Plenum Press, New York, 1-98, 1989

[72] Riis, S. K., Krogh, A. Improving prediction of protein secondary structure using structured neural networks and multiple sequence alignments. J. Comp. Biol. 3, 163-183, 1996

[73] Rose, G. D., Gierasch, L. M., Smith, J. A. Turns in peptides and proteins. Adv. Protein Chem. 37, 1109, 1985

[74] Rost, B., Sander, C. 1D secondary structure prediction through evolutionary profiles. In Protein Structure by Distance Analysis (Bohr, H., Brunak, S., eds.), 257-276, IOS Press, Amsterdam, Oxford, Washington, 1994

[75] Rost, B. PHD: predicting one-dimensional protein structure by profile based neural networks. Meth. Enzymol. 266, 525-539, 1996

[76] Rost, B. Better secondary structure prediction through more data. Columbia University, 2000, http://cubic.bioc.columbia.edu/predictprotein

[77] Rost, B., Eyrich, V.E. EVA: large-scale analysis of secondary structure prediction. Proteins, 45, 192-199, 2001

[78] Rumelhart, D. E., Hinton, G. E., Williams, R. J. Learning internal representations by error propagation. Parallel Distributed Processing, MA: MIT Press, Cambridge, 1(8), 318-362, 1986

[79] Salamov, A. A., Solovyev, V. V. Protein secondary structure prediction using local alignments. J. Mol. Biol. 268, 31-36, 1997

[80] Scholkopf, B., Burges, C. J. C., Smola, A. J. Advances in Kernel Methods: Support Vector Learning. MA: MIT Press, Cambridge, 1999

[81] Schonbrun, J., Wedemeyer, W. J., Baker, D. Protein structure prediction in 2002. Curr Op. in Str. Biol. 12, 348-354, 2002

[82] Shepherd, A. J., Gorse D., Thornton J. M. Prediction of the location and type of β-turns in proteins using neural networks. Protein Sci. 8, 1045 - 1055, 1999

[83] Shi, J., Blundell, T. L., Mizuguchi, K. FUGUE: Sequence-structure homology recognition using environment-specific substitution tables and structure-dependent gap penalties. J. Mol. Biol. 310, 243-257, 2001

[84] Szent-Gyrgyi, A. G., Cohen, C. Role of proline in polypeptide chain configuration of proteins. Science, 126, 697, 1957

[85] Taylor, W. R. Multiple protein sequence alignment: algorithms and gap insertion. Meth. Enzymol. 266, 343-367, 1996

[86] Thiele, R., Zimmer, R., Lengauer, T. Protein threading by recursive dynamic programming. J. Mol. Biol. 290, 757-779, 1999

[87] Thomas, P. D., Dill, K. A. An iterative method for extracting energy-like quantities from protein structures. Proc. Natl. Acad. Sci. USA, 93(21), 11628-11633, 1996

[88] Vapnik, V. Statistical Learning Theory. NY: Wiley, New York, 1998

[89] Venkatachalam, C. M. Stereochemical criteria for polypeptides and proteins. V. Conformation of a system of three linked peptide units. Biopolymers, 6, 14251436, 1968

[90] Vishwanathan, S. V. N., Smola, A. J. Fast Kernels for String and Tree Matching. Neural Information Processing Systems: Natural and Synthetic, Vancouver, Canada, 2002

[91] Vriend, G., WHAT IF: A molecular modeling and drug design program. J. Mol. Graph. 8, 52-56, 1990

[92] Wang, Z. X., Yuan, Z. How good is prediction of protein structural class by the component-coupled method. Proteins, 38(2), 165-175, 2000

[93] Wilmot, C. M., Thornton, J. M. Analysis and prediction of the different types of β-turn in proteins. J. Mol. Biol. 203(1), 221-32, 1988

[94] Zhang, C. T., Chou, K. C. Prediction of β-turns in proteins by 1-4 and 2-3 correlation model. Biopolymers, 41, 673-702, 1997

[95] Zhang, C. T., Chou, K. C. An optimization approach to predicting protein structural class from amino acid composition. Protein Sci. 1(3), 401-408, 1992

[96] Zvelebil, M. J., Barton, G. J., Taylor, W. R., Sternberg, M. J. E. Prediction of protein secondary structure and active sites using alignment of homologous sequences. J. Mol. Biol. 195, 957-961, 1987